Science of the Total Environment 756 (2021) 144009

Contents lists available at ScienceDirect

Science of the Total Environment

journal homepage: www.elsevier.com/locate/scitotenv

Geospatial analysis of COVID-19 lockdown effects on air quality in the South and Southeast Asian region

Sanjoy Roy [a,*], Monojit Saha [a,b], Bandhan Dhar [a,b], Santa Pandit [c], Rubaiya Nasrin [a,d]

[a] Bengal Institute for Architecture, Landscapes and Settlements, Dhaka, Bangladesh
[b] Dept. of Geography and Environment, University of Dhaka, Bangladesh
[c] United Nations University, Institute for the Advanced Study of Sustainability, Tokyo, Japan
[d] Urban and Regional Planning, Bangladesh University of Engineering and Technology, Dhaka, Bangladesh

HIGHLIGHTS

- Effects of COVID-19 lockdown measures on air quality were assessed at the regional-scale.
- National lockdown measures with effects on air quality were exclusively reviewed.
- Maximum reduction was noticed in tropospheric NO_2 column density.
- Dhaka, Kathmandu, Jakarta, and Hanoi exhibited the highest reduction in NO_2.
- An unexpected amplification in O_3 concentration was observed.

GRAPHICAL ABSTRACT

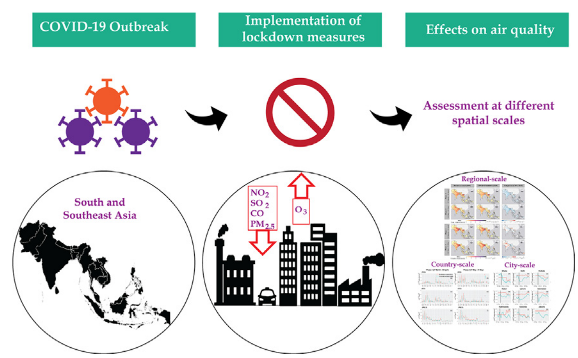

ARTICLE INFO

Article history:
Received 12 September 2020
Received in revised form 12 October 2020
Accepted 15 November 2020
Available online 21 November 2020

Editor: Philip K. Hopke

Keywords:
SARS-CoV-2
Air pollution
Satellite-based data
Lockdown setting

ABSTRACT

The COVID-19 pandemic, induced by the novel Coronavirus worldwide outbreak, is causing countries to introduce different types of lockdown measures to curb the contagion. The implementation of strict lockdown policies has had unprecedented impacts on air quality globally. This study is an attempt to assess the effects of COVID-19 induced lockdown measures on air quality in both regional, country, and city scales in the South and Southeast Asian region using open-source satellite-based data and software frameworks. We performed a systematic review of the national lockdown measures of 19 countries of the study area based on publicly available materials. We considered two temporal settings over a period of 66 days to assess and compare the effects of lockdown measures on air quality levels between standard business as usual and current situation COVID-19 lockdown. Results showed that compared to the same period of 2019, atmospheric NO_2, SO_2, $PM_{2.5}$, and CO levels decreased by an average of 24.16%, 19.51%, 20.25%, and 6.88%, respectively during the lockdown, while O_3 increased by a maximum of 4.52%. Among the 19 studied cities, Dhaka, Kathmandu, Jakarta, and Hanoi experienced the highest reduction of NO_2 (40%–47%) during the lockdown period compared to the corresponding period of 2019. The methodological framework applied in this study can be used and extended to future research in the similar domain such as understanding long-term effects of COVID-19 mitigation measures on the atmospheric pollution at continental-scale or assessing the effects of the domestic emissions during the stay-at-home; a standard and effective COVID-19 lockdown measure applied in most of the countries.

* Corresponding author at: Bengal Institute for Architecture, Landscapes and Settlements, Unique Oval, 45 Kamal Ataturk Avenue, Banani, Dhaka 1212, Bangladesh.
E-mail addresses: sroy.du@gmail.com (S. Roy), monojits76@gmail.com (M. Saha), bandhangeo@gmail.com (B. Dhar), pandit@unu.edu (S. Pandit), nasrinrubaiya@gmail.com (R. Nasrin).

https://doi.org/10.1016/j.scitotenv.2020.144009
0048-9697/

1. Introduction

The severe acute respiratory syndrome Coronavirus 2 (SARS-CoV-2), a novel coronavirus, caused a global health crisis with more than 760,774 deaths and almost 20.99 million confirmed cases as of August 15, 2020 (WHO, 2020a). The respiratory illness caused by this new coronavirus, commonly known as COVID-19, was first reported in Wuhan, China, in December 2019 (Acter et al., 2020; Ma et al., 2020; Wang et al., 2020c; Wu et al., 2020). As the number of confirmed cases increased in China and other parts of the world, on January 30, 2020, the World Health Organization (WHO) called for a global health emergency (Saadat et al., 2020). The spread of this highly contagious virus continued to increase, and the outbreak reported in 107 countries by March 11, 2020, when it was declared as a pandemic by the WHO (WHO, 2020b). The human-to-human transmissibility of the virus through infected respiratory droplets was confirmed as the primary way of contagion (Wang et al., 2020c; Wang et al., 2020b), and hence most of the countries imposed different levels of lockdowns over human activities ranging from local to nationwide to curb COVID-19 outbreak (Kaplan et al., 2020). The COVID-19 induced lockdown (C-19 lockdown) measures in most of the countries included social distancing, suspension of road and air traffic except the transportation of goods and emergency services, sealing of international borders, shutdown of industrial and commercial activities, and closure of educational institutes, wet markets, and restaurants (Anwar et al., 2020; Arunachalam and Halwai, 2020; Oxford Covid-19 Government Response Tracker, 2020; The Diplomat, 2020). The stringent imposition of such lockdown measures by the countries resulted in an enormous economic slowdown and social instability globally (Burke, 2020).

Though the COVID-19 pandemic has been considered as a significant reason for the current fall of the global economy, it has brought blessings to the environment. Already a number of studies showed unprecedented improvements in atmosphere and hydrosphere owing to a halt in human movement and economic activities during lockdown (Li et al., 2020; Muhammad et al., 2020; Mahato et al., 2020; Sharma et al., 2020b; Yunus et al., 2020; Zambrano-Monserrate et al., 2020). The reduction of pollutants in the atmospheres as an effect of C-19 lockdown could be observed all over the globe (atmospheric CO_2 concentration reduced by 6% globally) (Carbon Brief, 2020, as cited in Dutheil et al., 2020); however, there were marked differences noticed in different geographic settings. For instance, strict COVID-19 mitigation measures including social distancing had been enforced in China's Hubei Province at the end of 2019 to contain the spread of the virus, the economic activities including industries and power plant had stalled, resulting in a 40% and 20% drop in transportation and industrial emission, respectively (Wang et al., 2020c). Such measures also played significant role in the reduction of nitrogen dioxide (NO_2) and particulate matter 2.5 ($PM_{2.5}$) in several cities of China (ESA, 2020). According to CAMS (2020), several Chinese cities observed a 20–30% drop in the monthly average $PM_{2.5}$ concentrations in February 2020 compared to the same month in three previous years i.e., 2017, 2018, and 2019. Amid C-19 lockdown (in effect from January 23, 2020), Nichol et al. (2020) observed 60% and 80% reductions of tropospheric NO_2 concentration in Beijing-Tianjin-Hubei region in January and February 2020, compared with the same months of 2019. Lian et al. (2020) also found a marked reduction in NO_2 in most of Wuhan, China. In Spain, a decreasing trend in air pollution was observed just after two weeks of the imposition of lockdown measures -the average PM_{10} concentration decreased by 28–31% (Tobías et al., 2020). The partial lockdown of Sao Paulo, Brazil, resulted in 54.3% and 64.8% reduction in NO_2 and carbon monoxide (CO) levels in the air compared to the previous five years' monthly average values (Nakada and Urban, 2020). Likewise, the concentrations of $PM_{2.5}$, NO_2, and CO in the air decreased by 21%, 35%, and 49%, respectively in Almaty, Kazakhstan during C-19 lock-down (Kerimray et al., 2020). The Salé City of Morocco similarly experienced a significant drop in atmospheric NO_2, sulfur dioxide (SO_2), and PM_{10} concentrations during lockdown compared to the pre-lockdown period (Otmani et al., 2020). Satellite-based recent estimations of National Aeronautics and Space Administration (NASA) and European Space Agency (ESA) depicted at least 30% fall of air pollution in Spain, Italy, and the USA during COVID-19 pandemic (Muhammad et al., 2020).

Whereas the concentrations of NO_2, CO, SO_2, and $PM_{2.5}$ decreased in many parts of the world amid C-19 lockdown, few recent studies reported an unexpected increase in the atmospheric ozone (O_3) concentration, especially in the volatile organic carbon-limited (VOC-limited) regimes. For example, an approximately 50% increase in O_3 concentration was recorded in the urban center of Barcelona (Spain) during the lockdown (Tobías et al., 2020). Wang et al. (2020d) estimated around 145% and 46% increase in O_3 concentration in the urban and rural areas of Hangzhou (China), respectively. In the VOC-limited region of Rajasthan (India), a maximum 45% increase in O_3 concentration was observed during the lockdown (Sharma et al., 2020b). Likewise, Sicard et al. (2020) estimated an approximately 17% increase in O_3 concentration in the four European cities (Nice, France; Rome and Turin, Italy; and Valencia, Spain) and 36% in Wuhan, China during the lockdown (2020) compared to the same period of 2017–2019. The exacerbation in O_3 concentration during the restricted anthropogenic emission period (C-19 lockdown) was also confirmed by Le et al. (2020). These studies mainly highlighted the reduction in NO_2 emission, due to the limited operations of the emission sources during the lockdown, as one of the most important reasons for increasing O_3 concentration. In the troposphere, O_3 mainly forms by the reaction between atmospheric nitrogen oxides (NO_x) and VOCs with the presence of effective solar radiation (Seinfeld and Pandis, 1998). But the reduced NO_x emissions during the lockdown lowered the O_3 titration by NO and increased the VOC-NO_x ratio, which basically amplified O_3 concentration in the lower atmosphere during C-19 lockdown (Sicard et al., 2020). However, this increase of O_3 in the lower atmosphere may cause serious health problems to humans (Dang and Liao, 2019; Lefohn et al., 2018).

The outbreak of the coronavirus in South (SA) and Southeast Asian (SEA) region was confirmed on mid-January 2020. Since then, the confirmed cases began to increase swiftly in SA and SEA countries. Surprisingly, the case fatality in this region is much lower than in Europe and North America (BI, 2020). From the date of the first record, a total of 3,516,456 confirmed cases with 68,995 deaths were recorded in this region as of August 15, 2020, while only five countries such as India, Pakistan, Bangladesh, Philippines, and Indonesia together accounted for 95.97% of confirmed cases and 97.47% of total deaths (WHO, 2020a). Restraining the rapid spread of COVID-19 was a major concern for the SA and SEA countries, and thereby numerous mitigation measures such as restricting public gathering, social distancing, closing international borders, limiting people's movement, quarantine affected areas, etc. were adopted.

Along with these common measures, most of the SA and SEA countries enforced community-wise to nationwide lockdown measures. The effects of the implementation of such measures on air quality in a few SA and SEA countries have been studied so far, which showed a substantial decrease in NO_2, SO_2, PM, and CO concentrations and an unexpected increase in O_3 concentration during the C-19 lockdown. For example, Kanniah et al. (2020) found a 27–34% reduction in tropospheric NO_2 column density in the urban agglomerations of SEA with a notable decrease in PM_{10}, $PM_{2.5}$, CO, and SO_2 levels in the urban areas of Malaysia during COVID-19 period of 2020 compared to the mean of 2015–2019. During the lockdown phase, Delhi, the capital city of India observed 60%, 30%, 52.68%, and 30.35% reductions in PM_{10}, $PM_{2.5}$, NO_2, and CO concentrations, respectively, compared to the same period of 2019 (Mahato et al., 2020). Likewise, Mandal and Pal (2020) found three to four times a reduction in the concentration of PM_{10} at the stone quarrying and crushing locations in the Dwarka river basin of Eastern India after the imposition of lockdown. The cutbacks in $PM_{2.5}$, PM_{10}, CO, and NO levels during lockdown were also proven in six megacities of India (Jain and Sharma, 2020). On the other hand, a study conducted over 22 cities of India identified a significant rise in O_3 concentration during the lockdown period (CES, 2020). Although these studies provided quantitative information about the changes of air quality amid C-19 lockdown in India, Malaysia, and few urban areas of SEA, the effects of lockdown on regional-scale air quality are still inadequate.

Being one of the most populated and industrialized areas in the world, improvements in air quality across the SA and SEA regions during the COVID-19 lockdown period ought to be explored to consider the possible ways of mitigation of air pollution at the regional level. Therefore, this study aims to assess the effects of COVID-19 induced lockdown measures on five different air pollutants across 19 countries of the SA and SEA regions. To our knowledge, this is the first regional-scale assessment that also explored the change of air quality at country and city scales to provide a comprehensive overview of the effects of COVID-19 lockdown on regional air quality in the study area.

2. Material and methods

2.1. Description of the study area

Being one of the higher air polluted regions in the world, all 19 countries of South Asia (8 countries) and Southeast Asia (11 countries) were selected to perform a regional scale assessment of the effects of COVID-19 lockdown on air quality (Fig. 1). The study area covers 11 million km^2, which is 24.84% of entire Asia. It contains almost one-third of the world's population (32.55%) with a density of 225.54/km^2, where the population density of SA (288/km^2) is twice that of Southeast Asia (SEA) (140.82/km^2; The World Bank, 2019). According to the World Bank, 2019 Indicator List, all 17 countries of the study area fall in the lower to upper-middle-income groups except Brunei Darussalam and Singapore (Annex I). The World Development Indicators List (2019) shows a growing economy in these countries with positive annual growth of GDP (Annex II) aided by rapid industrial and infrastructural development. With the increasing economic development, this region has been experiencing severe air pollution since the last decades. In many countries, the emission of several pollutants induced from burning of biomass in the crop fields, combustion of fuels in power plants and vehicles, industries operations, and domestic consumptions exceeds the limits set by the World Health Organization (WHO) (WHO, 2006; Bhattacharya, et al., 2000; John et al., 1999, Hopke et al., 2008). For example, the annual average PM_{10} concentrations in Lahore and Rawalpindi were estimated as 368 μg/m^3 and 276 μg/m^3, respectively, which are excessively higher than the WHO standard (20 μg/m^3) (Ghauri et al., 2007). According to Ilyas et al. (2010), suspended particulate matter (SPM), respirable particulate matter (RPM), SO_2, NO_x, lead (Pb), and CO_2 in the atmosphere of Pakistan are consistently higher than the tolerable range. In Bangladesh, the concentration of several pollutants notoriously exceed the standard levels in the dry seasons of the year (Motalib et al., 2015; Rahman and Al-Muyeed, 2005; Zahangir et al., 2001). The level of air pollution in India is so high that it has been identified as one of the primary reasons for premature death (WHO, 2014). Similarly, in SEA countries, the level of air pollution is observed above the standard level, where the Air Quality Index (AQI) in the major cities remains unhealthy in most of the days of the year (Luong et al., 2019). Few SEA cities such as Bandung, Manila, and Hanoi have been experiencing high concentrations of $PM_{2.5}$ and PM_{10} (Oanh et al., 2006). In the SEA region, Myanmar, Vietnam, Indonesia, and Laos have been facing tremendous air pollution compared to other countries (IQAir, 2019). However, few countries such as Malaysia, Singapore, Thailand, Philippines, and Cambodia have set several national guidelines, which are effective in maintaining good air quality status (Southeast Asia air quality regional report, UNEP).

COVID-19 contagion in the study area was first recorded on January 13, 2020 in Thailand (WHO, 2020c). In the SA region, it was first

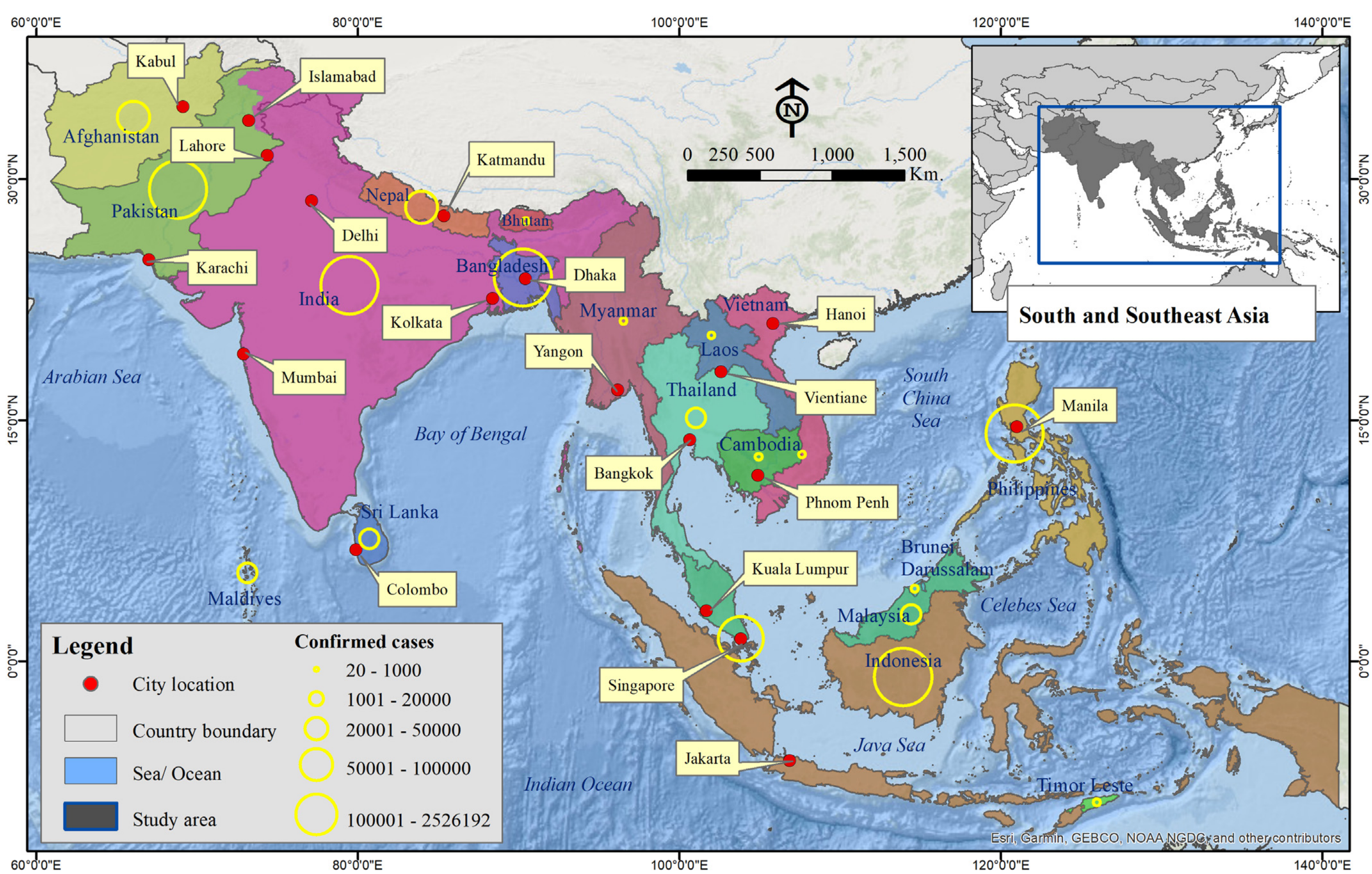

Fig. 1. South and Southeast Asian countries with selected major cities and COVID-19 confirmed cases as of August 15, 2020.

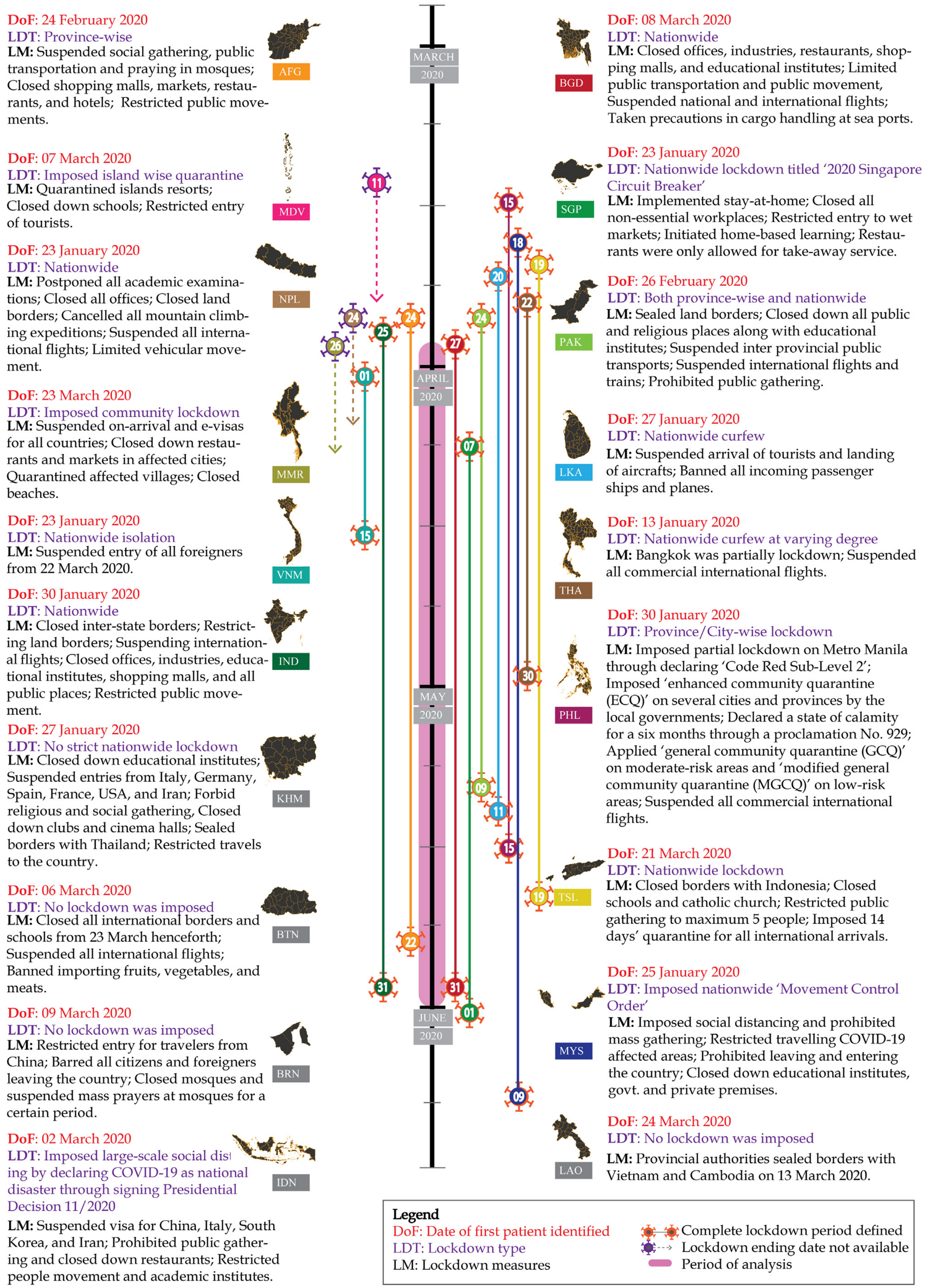

DoF: 24 February 2020
LDT: Province-wise
LM: Suspended social gathering, public transportation and praying in mosques; Closed shopping malls, markets, restaurants, and hotels; Restricted public movements.
AFG
DoF: 07 March 2020
LDT: Imposed island wise quarantine
LM: Quarantined islands resorts; Closed down schools; Restricted entry of tourists.
MDV
DoF: 23 January 2020
LDT: Nationwide
LM: Postponed all academic examinations; Closed all offices; Closed land borders; Cancelled all mountain climbing expeditions; Suspended all international flights; Limited vehicular movement.
NPL
DoF: 23 March 2020
LDT: Imposed community lockdown
LM: Suspended on-arrival and e-visas for all countries; Closed down restaurants and markets in affected cities; Quarantined affected villages; Closed beaches.
MMR
DoF: 23 January 2020
LDT: Nationwide isolation
LM: Suspended entry of all foreigners from 22 March 2020.
VNM
DoF: 30 January 2020
LDT: Nationwide
LM: Closed inter-state borders; Restricting land borders; Suspending international flights; Closed offices, industries, educational institutes, shopping malls, and all public places; Restricted public movement.
IND
DoF: 27 January 2020
LDT: No strict nationwide lockdown
LM: Closed down educational institutes; Suspended entries from Italy, Germany, Spain, France, USA, and Iran; Forbid religious and social gathering, Closed down clubs and cinema halls; Sealed borders with Thailand; Restricted travels to the country.
KHM
DoF: 06 March 2020
LDT: No lockdown was imposed
LM: Closed all international borders and schools from 23 March henceforth; Suspended all international flights; Banned importing fruits, vegetables, and meats.
BTN
DoF: 09 March 2020
LDT: No lockdown was imposed
LM: Restricted entry for travelers from China; Barred all citizens and foreigners leaving the country; Closed mosques and suspended mass prayers at mosques for a certain period.
BRN
DoF: 02 March 2020
LDT: Imposed large-scale social distancing by declaring COVID-19 as national disaster through signing Presidential Decision 11/2020
LM: Suspended visa for China, Italy, South Korea, and Iran; Prohibited public gathering and closed down restaurants; Restricted people movement and academic institutes.
IDN
MARCH 2020
APRIL 2020
MAY 2020
JUNE 2020
DoF: 08 March 2020
LDT: Nationwide
LM: Closed offices, industries, restaurants, shopping malls, and educational institutes; Limited public transportation and public movement, Suspended national and international flights; Taken precautions in cargo handling at sea ports.
BGD
DoF: 23 January 2020
LDT: Nationwide lockdown titled '2020 Singapore Circuit Breaker'
LM: Implemented stay-at-home; Closed all non-essential workplaces; Restricted entry to wet markets; Initiated home-based learning; Restaurants were only allowed for take-away service.
SGP
DoF: 26 February 2020
LDT: Both province-wise and nationwide
LM: Sealed land borders; Closed down all public and religious places along with educational institutes; Suspended inter provincial public transports; Suspended international flights and trains; Prohibited public gathering.
PAK
DoF: 27 January 2020
LDT: Nationwide curfew
LM: Suspended arrival of tourists and landing of aircrafts; Banned all incoming passenger ships and planes.
LKA
DoF: 13 January 2020
LDT: Nationwide curfew at varying degree
LM: Bangkok was partially lockdown; Suspended all commercial international flights.
THA
DoF: 30 January 2020
LDT: Province/City-wise lockdown
LM: Imposed partial lockdown on Metro Manila through declaring 'Code Red Sub-Level 2'; Imposed 'enhanced community quarantine (ECQ)' on several cities and provinces by the local governments; Declared a state of calamity for a six months through a proclamation No. 929; Applied 'general community quarantine (GCQ)' on moderate-risk areas and 'modified general community quarantine (MGCQ)' on low-risk areas; Suspended all commercial international flights.
PHL
DoF: 21 March 2020
LDT: Nationwide lockdown
LM: Closed borders with Indonesia; Closed schools and catholic church; Restricted public gathering to maximum 5 people; Imposed 14 days' quarantine for all international arrivals.
TSL
DoF: 25 January 2020
LDT: Imposed nationwide 'Movement Control Order'
LM: Imposed social distancing and prohibited mass gathering; Restricted travelling COVID-19 affected areas; Prohibited leaving and entering the country; Closed down educational institutes, govt. and private premises.
MYS
DoF: 24 March 2020
LDT: No lockdown was imposed
LM: Provincial authorities sealed borders with Vietnam and Cambodia on 13 March 2020.
LAO
Legend
DoF: Date of first patient identified
LDT: Lockdown type
LM: Lockdown measures
Complete lockdown period defined
Lockdown ending date not available
Period of analysis

reported on January 23, 2020 in Nepal (Shrestha et al., 2020). Afterward, all other countries of SA reported COVID-19 infections by March 8, 2020 (BI, 2020; WHO, 2020a). After the first case was reported in Thailand, the contagion spread in all other SEA countries by March 24, 2020. To contain the spread of the virus, all the countries of the study area imposed several types and levels of lockdown measures, mostly on different dates of March 2020, which included nationwide shut down of economic activities, restrictions in social gathering, suspension of vehicular movements, etc.

2.2. Review of country-based COVID-19 lockdown measures with effects on air quality

A systematic review of the national lockdown measures was performed for all the countries based on their national health directorate resolutions, ministerial declarations, published literature, and national and international newspapers (Annex III). Since several countries published COVID-19 guidelines and contingency measures in their official language other than English, we had to rely mostly on the English newspapers for collecting and collating information. The review was performed from the day of the first reported case for an individual country to the May 31, 2020. After compilation of country-based lockdown measures, these were filtered, and the most relevant measures were considered, which can affect the levels of pollutants in the atmosphere (Fig. 2). Except for Singapore (SGP), all other countries of the study area imposed lockdown on different dates of March 2020. A significant variation in lockdown type was observed from country to country in the study. In SA, all the countries except Afghanistan (AFG) and Maldives (MDV) imposed nationwide lockdown from the fourth week of March to the end of May. AFG followed province-wise lockdown based on the number of contagions. MDV quarantined different islands, especially the most touristic ones where the infections were reported. Bhutan (BTN) didn't follow stringent lockdown rather restricted mass gathering and postponed all international flights. In SEA, Laos (LAO), Cambodia (KHM), and Brunei Darussalam (BRN) didn't apply any sort of lockdown but restricted social gathering, closed educational institutes, suspended entry of travelers from the COVID-19 affected countries, and sealed borders with the neighboring states. The other eight countries applied different types of lockdown, ranging from community lockdown (Myanmar-MMR) to nationwide curfew (Thailand-THA).

Indonesia (IDN) declared the pandemic as a national disaster and thereby imposed large-scale social distancing through a presidential decision 11/2020. Under this type of contingency measure, IDN suspended international flights with profoundly affected countries, restricted vehicular movements for controlling human movement, and closed restaurants. Similar measures were imposed in Malaysia (MYS) and Vietnam (VNM) under the titles 'Movement Control Order' and 'Nationwide Isolation', respectively. SGP officially imposed lockdown measures a bit later than the date of the first record (January 23, 2020) compared to the other SEA countries. On April 7, 2020, SGP imposed a nationwide lockdown with the title '2020 Singapore Circuit Breaker' under which it closed down all non-essential workplaces and tightly implemented stay-at-home order for the residents. Timor-Leste (TSL) additionally implemented a 14-days mandatory quarantine for the international arrivals with other standard measures under the nationwide lockdown. On the other hand, Philippines (PHL) imposed three different types of community quarantines depending on the COVID-19 risk levels of the cities or areas.

Along with the partial lockdown of the Metro Manila, PHL declared the pandemic as a state calamity under Proclamation No. 929 and suspended all national and international flights. From Fig. 2 it can be summarized that most of the countries imposed similar lockdown measures for containing the spread of SARS-CoV-2 virus in the study region. Among all the measures, most of the countries suspended road and air transports, closed down industrial and processing activities, and limited construction works, which are considered as the primary point sources of air pollution in the study area.

2.3. Satellite-based estimations of air pollutants used in the study

Satellite-based measurements of air pollutants are widely used by researchers, policymakers, and environmentally conscious private and public entities (Duncan et al., 2014, Fioletov, et al., 2011). The insufficiency of ground stations around the world is a major reason for the increasing popularity of satellite-based estimations usage in monitoring air quality (Zou et al., 2017). In this study, satellite observation-based reanalysis data and satellite-based measurements were used to monitor the effect of COVID-19 lockdown measures on the levels of NO_2, SO_2, CO, $PM_{2.5}$, and O_3 in the atmosphere. For extracting the geospatial dataset, we used the Goddard Interactive Online Visualization and Analysis Infrastructure (GIOVANNI) (https://giovanni.gsfc.nasa.gov/giovanni/), which provides both reanalyzed model outputs and surface observations on the several air quality parameters (Prados et al., 2010). The time average of SO_2 (column mass density), CO (surface concentration and near-source emission), and $PM_{2.5}$ (dust column mass density) gridded dataset of the Modern-Era Retrospective Analysis for Research and Applications Version 2 (MERRA-2) model with $0.5° \times 0.625°$ spatial and hourly (SO_2 and $PM_{2.5}$)/monthly (CO) temporal resolutions were extracted for two-time frames (March 27–April 30 and May 1–May 31) of 2019 and 2020. The MERRA-2 model is an atmospheric reanalysis which uses the Goddard Earth Observing System Model v.5 (GEOS-5) coupled with the Atmospheric Data Assimilation System (ADAS) (GMAO, 2015). The time average of NO_2 (tropospheric column density) and O_3 (total column concentration) along with weekly average of NO_2 (tropospheric column density) having $0.25° \times 0.25°$ spatial and hourly (NO_2)/daily (O_3) daily temporal resolutions for the same time frames of the respective years were extracted from the Ozone Monitoring Instrument of the NASA Aura satellite (OMI/Aura) level-3 daily global gridded product (Nickolay et al., 2019). Furthermore, we used the monthly average (March to May) of surface wind speed (m/s) geospatial dataset with $2.5° \times 2.5°$ spatial and monthly temporal resolutions for the years of 2019 and 2020 extracted from the NCEP/NCAR Reanalysis (https://psl.noaa.gov/data/gridded/data.ncep.reanalysis.html) (Kalnay et al., 1996) for understanding the variation of surface wind speed between the study periods which could affect the vertical movement of emissions. The specific properties of the dataset used in the study are provided in Table 1.

2.4. Temporal settings used in the study

The air pollutants were compared between two temporal frames over a period of 66 days (March 27 to May 31). This time period was considered because the lockdown was in effect during this period in most of the countries of the study area.

Fig. 2. Country-based COVID-19 reported dates and lockdown measures with effects on air pollution in the study area. The ISO Alpha-3 country code (https://www.iso.org/) for the respective countries were used instead of their full names. This figure was developed through a comprehensive review of country-based COVID-19 induced lockdown measures, as presented in Annex III. Lockdown periods for respective countries were presented on a time axes with solid lines of different colors corresponding to the colors of the country names. The numeric values on the time axes lines represented the starting and ending dates of lockdown of the individual countries. Note: AFG — Afghanistan; BGD — Bangladesh; IND — India; PAK — Pakistan; NPL — Nepal; BTN — Bhutan; LKA — Sri Lanka; MDV — Maldives; MMR — Myanmar; THA — Thailand; IDN — Indonesia; MYS — Malaysia; VNM — Vietnam; KHM — Cambodia; LAO — Laos (Lao PDR); BRN — Brunei Darussalam; SGP — Singapore; TSL — Timor-Leste; PHL — Philippines.

Table 1
Geospatial dataset with their different attributes used in the study.

Data used	Data type	Spatial resolution	Temporal resolution	Unit	Sensor/model	Source
Nitrogen dioxide (NO_2)	Tropospheric column density	0.25° × 0.25°	Hourly	molecule/cm^2	AURA OMI	https://earthdata.nasa.gov/
Sulfur dioxide (SO_2)	Column mass density	0.5° × 0.625°	Hourly	kg/m^2	MERRA-2 Model	
Particulate matter ($PM_{2.5}$)	Dust column mass density	0.5° × 0.625°	Hourly	kg/m^2	MERRA-2 Model	
Carbon monoxide (CO)	Surface concentration	0.5° × 0.625°	Monthly	ppbv	MERRA-2 Model	
Carbon monoxide (CO)	Near source emission	0.5° × 0.625°	Monthly	kg/m^2 s	MERRA-2 Model	
Ozone (O_3)	Total column concentration	0.25° × 0.25°	Daily	Dobson Unit (DU)	AURA OMI	
Wind speed	Surface wind	2.5° × 2.5°	Monthly	m/s	NCEP/NCAR Reanalysis	https://psl.noaa.gov/

1) *Business as usual (BAU) setting*: The period between March 27 and May 31, 2019 was considered as the business as usual (BAU) with the normal setting of economic activities.
2) *COVID-19 lockdown (C-19) setting*: The period between March 27 and May 31, 2020 was considered as the COVID-19 lockdown (C-19), attributed by a new-normal setting of economic activities.

The analysis period (March 27 to May 31) was further divided into two sub-periods: Phase-1 (P1 — March 27 to April 30) and Phase-2 (P2 — May 1 to May 31), for understanding the changes in air pollutant levels between these phases as few countries relaxed the lockdown measures and resumed transportation and few economic activities during phase-2. This phasing scheme can be applied independently for most of the countries in the study area except those which had no lockdown ending dates available.

2.5. Data processing and analysis

The geospatial datasets extracted from the GIOVANNI and the NCEP/NCAR Reanalysis were initially projected to the WGS1984 geographic coordinates, which were re-projected to the WGS1984-World Mercator for facilitating spatial analysis. The spatial resolution of the datasets was resampled to 1 km using the nearest neighbor resampling method and clipped to the study area boundary. The analysis was performed at the following three spatial scales.

1) *Regional-scale*: In the regional-scale analysis, each pollutant dataset of C-19 lockdown phases was compared with that of the BAU phases using left-tailed *t*-test. The *t*-test was performed to confirm if the regional mean of an individual pollutant during the C-19 lockdown setting was lower than the regional mean of the same pollutant in BAU setting. In the *t*-test procedure, the statement '*regional mean of X-pollutant in C-19 < regional mean of X-pollutant in BAU*' was considered as the alternative hypothesis and the *P*-value for each comparison was calculated at 95% confidence interval. Additionally, the temporal difference maps were generated to quantify the area and level of changes of the pollutants at each phase.
2) *Country-scale*: In the country-scale analysis, the comparisons of the pollutants were performed for each country between C-19 and BAU settings at the respective phases.
3) *City-scale*: For city-scale analysis, 19 highly air polluted cities were selected from the study area based on the World Air Quality Report, 2019 (IQAir, 2019). The weekly average datasets of the NO_2 were used to extract the mean values for the cities. Finally, the weekly NO_2 mean values of the cities were compared between C-19 and BAU settings.

3. Results and discussion

3.1. Effects on air quality across South and Southeast Asian region

The geospatial distribution of atmospheric NO_2, SO_2, $PM_{2.5}$, CO, and O_3 levels during BAU and C-19 lockdown settings are presented in Figs. 3 and 4 (column 1 and column 2). The right-side columns (column 3) in both figures (Figs. 3 and 4) represent the change of the pollutants between C-19 and BAU temporal settings at two different phases. The comparison of the regional mean values of air pollutants between C-19 and BAU settings using left-tailed *t*-test confirmed that the average levels of NO_2, SO_2, and $PM_{2.5}$ in the atmosphere of the study area reduced during the C-19 lockdown compared to the average levels of the corresponding BAU ($p < 0.05$) (Annex IV). But the average CO and O_3 concentrations increased in the study area during the C-19 lockdown setting ($p > 0.05$) despite different lockdown measures were implemented.

Results obtained from the map difference showed varying percentages of the reduction of pollutants in the atmosphere at both spatial extents and temporal frames. Within the study periods, a minimum of 23.73% to a maximum of 86.28% of the entire study area experienced an overall decrease in NO_2, SO_2, CO, and $PM_{2.5}$ levels during the C-19 lockdown period compared to the same period of BAU (Table 2). The decline was noticed for all three estimates (minimum, maximum, and mean) of the pollutants with the progression of the enforcement of C-19 lockdown measures. As shown in Table 2, the maximum spatial extent of reduction was observed in $PM_{2.5}$ (75.77% area in P1 and 86.28% area in P2), followed by NO_2 (62.18% area in P1 and 72.89% area in P2) and SO_2 (74% area in P1 and 56.35% area in P2). The NO_2 showed the highest average reduction (21.86% to 24.16%) (Fig. 3c and f) by value, followed by $PM_{2.5}$ (17.94% to 20.25%) (Fig. 3o and r) and SO_2 (14% to 19.51%) (Fig. 3i and l) in the C-19 lockdown period compared to the corresponding BAU period.

Though CO showed an overall increase throughout the study area during the C-19 lockdown period as compared with the BAU period, it still exhibited a 5.45% to 6.88% reduction (Table 2) of surface concentration in 23.73% to 51.02% area of the entire study area (Fig. 4c and f). The near-source emission data also represented a reduction of CO emission from the sources during the lockdown (Fig. 4i and l). On the contrary, 53% (Fig. 4r) to 80% (Fig. 4o) of the study area exhibited an exacerbation in O_3 concentration during the same comparison period, where a maximum of 4.5% mean increase (270.16 DU to 282.37 DU) was noticed in P1 in the entire study area (Table 2). The spatial extent of elevated O_3 concentration gradually decreased over time, yet there was an increase in 53% of the study area in P2. However, with the exception of CO and O_3, the regional average reduction of all other pollutants accelerated during the P2 compared to the P1.

The suspension of public transportation, shut down of industries and other emission sources, and standstill of construction activities during C-19 lockdown are the significant causes behind such reduction of NO_2, SO_2, CO, and $PM_{2.5}$ in the atmosphere of the study area. For example, more than 50% of textile production declined in India (84.26%), Malaysia (52.08%), Singapore (82.67%), and Sri Lanka (84.52%) during C-19 lockdown (April 1 to May 31, 2020) compared to the same BAU period (2019). Similarly, food production and processing, chemicals, and manufacturing industries of these countries exhibited a significant reduction in production as affected by the execution of C-19 mitigation measures (Annex V). Google-based data on human mobility in the public transport hubs, as a proxy of road traffic, showed a decreasing trend of human movement in the countries of the study area in March, April, and May of 2020 with comparison to the corresponding months of 2019. The countries exhibited the highest reduction of human mobility in April, as most of the countries imposed firm nationwide suspension over vehicular

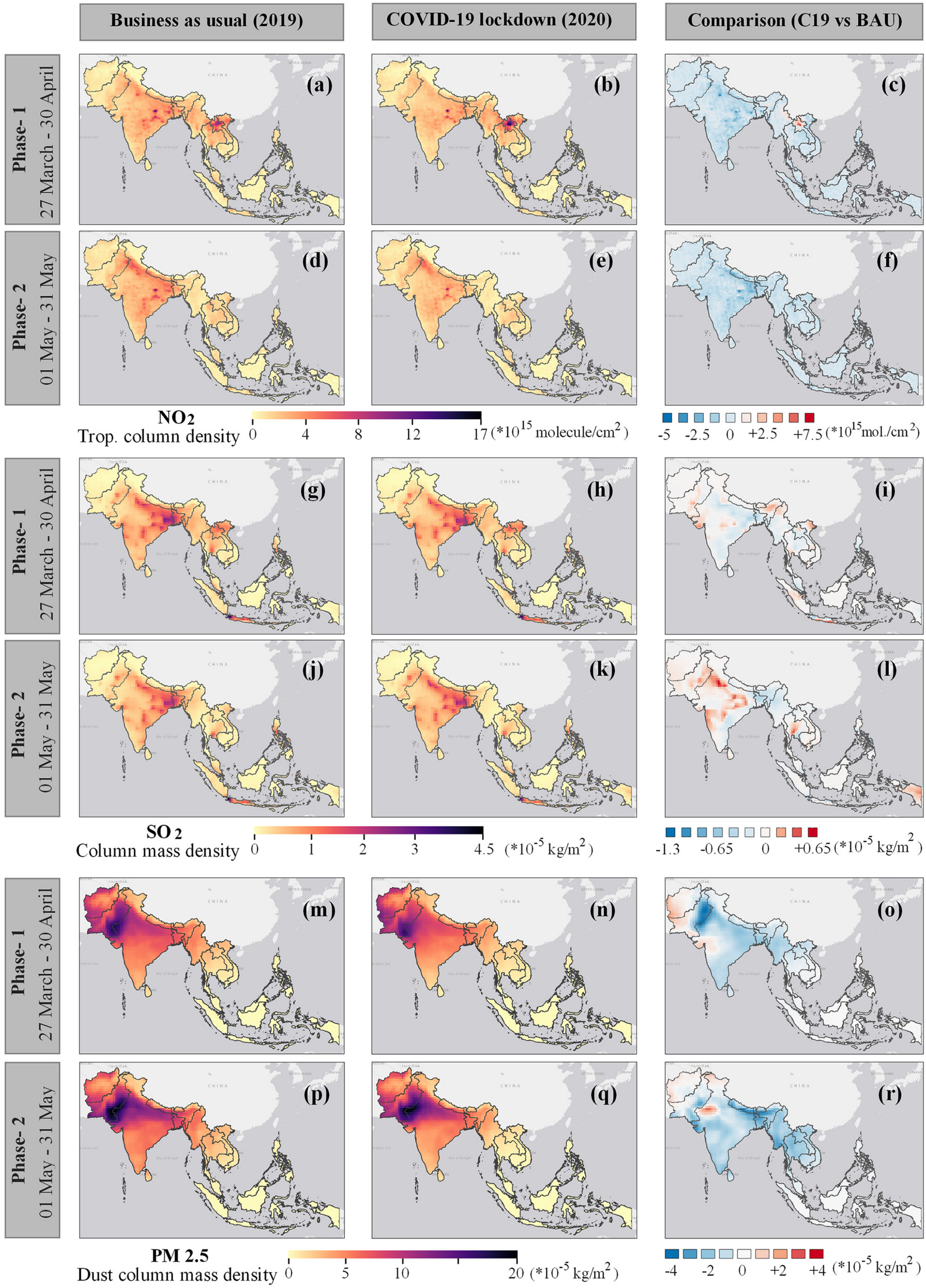

Fig. 3. Geospatial distribution of atmospheric NO_2, SO_2, and $PM_{2.5}$ column densities in the study area at two phases (Phase-1 and Phase-2) during BAU (March 27–May 31, 2019) and C-19 lockdown (March 27–May 31, 2020) settings (column 1 and column 2). Column 3 represents the comparison of the pollutants between C-19 lockdown and BAU temporal frames.

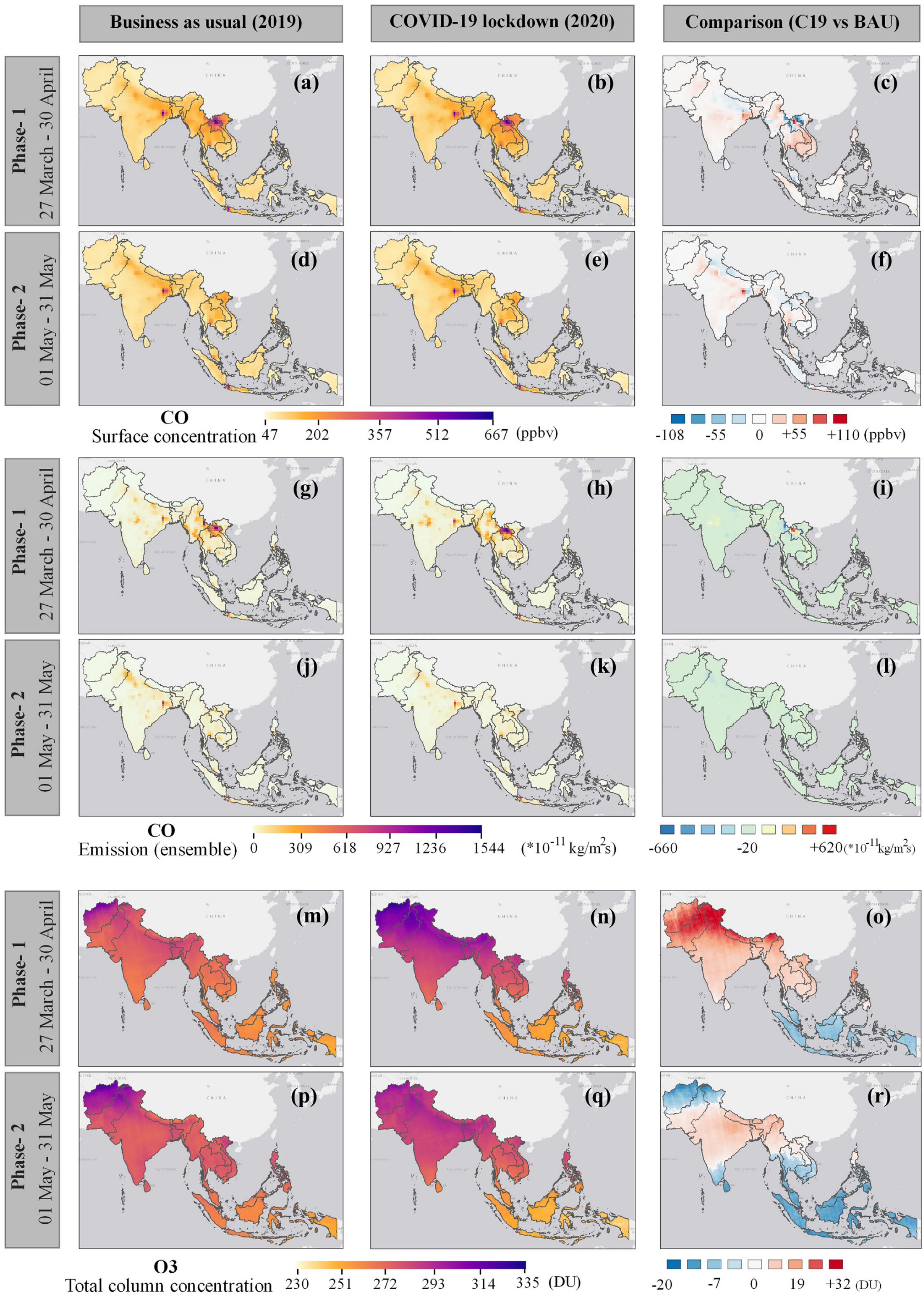
Business as usual (2019)
COVID-19 lockdown (2020)
Comparison (C19 vs BAU)
Phase- 1
27 March - 30 April
Phase- 2
01 May - 31 May
(a)
(b)
(c)
(d)
(e)
(f)
CO
Surface concentration
47 202 357 512 667 (ppbv)
-108 -55 0 +55 +110 (ppbv)
(g)
(h)
(i)
(j)
(k)
(l)
CO
Emission (ensemble)
0 309 618 927 1236 1544 (*10-11 kg/m2s)
-660 -20 +620(*10-11kg/m2s)
(m)
(n)
(o)
(p)
(q)
(r)
O3
Total column concentration
230 251 272 293 314 335 (DU)
-20 -7 0 19 +32 (DU)

Table 2
Regional statistics of the pollutants and their mean differences during the C-19 lockdown setting (2020) compared to the BAU setting (2019). Min and max are the representations of minimum and maximum values of the pollutants throughout the study area.

Pollutants	Phases	Change by area (%)	BAU			C-19			Mean difference (%)
			Min	Max	Mean	Min	Max	Mean	
CO	P1	−23.73	54.17	580.01	129.98	53.95	478.89	121.04	−6.88
	P2	−52.05	48.82	531.13	92.23	48.37	476.58	87.2	−5.45
NO_2	P1	−62.18	0	12.98	1.83	0	11.25	1.43	−21.86
	P2	−72.89	0	13.97	1.78	0	11.38	1.35	−24.16
SO_2	P1	−74	0.01	3.93	0.5	0.01	3.54	0.43	−14.00
	P2	−56.35	0.02	4.33	0.41	0.02	3.59	0.33	−19.51
$PM_{2.5}$	P1	−75.77	0.07	17.42	4.85	0.05	16.09	3.98	−17.94
	P2	−86.28	0.02	19.71	4.89	0.02	19.66	3.9	−20.25
O_3	P1	80	239.55	314.42	270.16	237.13	330.23	282.37	4.52
	P2	53	243.52	323.07	275.51	234.02	306.10	276.03	0.19

movement by the end of March 2020 to contain the spread of the virus. For example, Bangladesh, Laos, Malaysia, Nepal, Philippines, and Sri Lanka experienced an above 60% reduction of human movement through public transports in April 2020 compared to April 2019 (Annex VI). Global air traffic frequency has been worst affected due to the suspension of national and international flights by the countries as one of the vital measures to restrain the contagion of the new Coronavirus. Amid COVID-19 pandemic, global scheduled flights reduced 65.9% and 68.9% in April and May of C-19 lockdown compared to the same months of BAU (OAG Schedules Analyser, 2020). In South Asian flights, 30% and 35% scheduled seats reduced in April and May 2020, respectively, compared to the same months of 2019. On the other hand, Southeast Asian flights faced a fall of scheduled seats by 50% in April and 55% in May 2020 compared to the corresponding months of the previous year (Annex VII).

While atmospheric NO_2, $PM_{2.5}$, SO_2, and CO exhibited some degree of decrease in both spatial extent and concentration when compared to BAU at both phases of lockdown, an opposite scenario was noticed in atmospheric O_3 concentration as explained earlier in this section. This finding from our research is aligned with other recent literature published on different study areas (CSE, 2020; Le et al., 2020; Lian et al., 2020; Sicard et al., 2020; Sharma et al., 2020b; Wang et al., 2020d). While all these studies recorded an increase in O_3 concentrations during the lockdown period, the reason for this increase was attributed differently. Le et al. (2020) explained this increase as a result of the alleviated titration of O_3 by NO during the lockdown over the VOC-limited regime. A similar explanation was given by Tobías et al. (2020), which further added the decreased emission of NO_2 in the VOC-limited environment during the lockdown as a factor for increased O_3 in the lower atmosphere. Other studies also concluded that the temporarily shut down of the major sources of $PM_{2.5}$ and NO_2 emission during the lockdown period accelerated the photochemical reaction producing extra O_3 in the lower atmosphere under increased solar radiation due to decreased $PM_{2.5}$ and in addition to decreased NO_2 concentration (CSE, 2020; Hu et al., 2017; Jhun et al., 2014; Sharma et al., 2020b). Our study also confirmed a considerable reduction of NO_2 and $PM_{2.5}$ levels in the C-19 lockdown, which might enhance the photochemical reaction due to increased solar radiation in the clean atmosphere and thereby have resulted in increased production of O_3 concentration in our study area during this lockdown. However, meteorological factors such as temperature, wind speed, relative humidity, and water vapor pressure may affect the exacerbation of O_3 concentration in the atmosphere (Kovač-Andrić et al., 2013). Therefore, we conclude that the reasons behind increased O_3 during the C-19 lockdown situation need to be investigated further involving meteorological factors to reach a conclusion about the attributing mechanism.

3.2. Effects on air quality in SA and SEA countries

We estimated the country-wise changes in air pollution levels during C-19 lockdown (2020) compared to BAU (2019) at two analytical phases. The findings revealed significant improvement of air quality in most of the countries during the C-19 lockdown as they exhibited a considerable decline in the levels of air pollutants at both phases compared to the corresponding phases of BAU (Fig. 5).

The countries that enforced tight nationwide lockdown measures for an extended period, exhibited a higher reduction of atmospheric NO_2 levels in both phases of C-19 lockdown compared to the same phases of the previous year. For example, SGP, NPL, BGD, IND, and PAK imposed a stringent nationwide lockdown for the entire study period under which they postponed all national and international flights, shut down industrial and processing sectors, restricted road traffic, and suspended construction activities (Fig. 2). Therefore, these countries observed 8.63% (PAK) to 48.71% (SGP) fall in average NO_2 column density during lockdown as compared to BAU. Some other countries, which implemented province-wise to city-wise lockdown measures also experienced a reduction in average NO_2 such as VNM, MDV, and PHL. The countries that didn't impose strict lockdown over emission activities instead moved towards the implementation of more common measures such as restricted social gathering, sealed borders with neighbors, and closed down academic institutes, observed the least reduction in atmospheric NO_2 level. Results obtained from the analysis of 19 countries showed that the average NO_2 column density reduced in 16 countries during the phase-1 (27 March to 30 April) of C-19 lockdown, when the maximum reduction was observed in SGP (48.71%, -2.63×10^{15} molecules/cm^2) followed by NPL (−18%, -0.29×10^{15} molecules/cm^2), IND (−17.41%, -0.39×10^{15} molecules/cm^2), BGD (−11.40%, -0.31×10^{15} molecules/cm^2), and MDV (−10.25%, -0.02×10^{15} molecules/cm^2) (Fig. 5a). A similar scenario was observed in phase-2 with an accelerated trend of reduction in few countries, particularly the countries that continued an uninterrupted lockdown for a prolonged period. Such countries include NPL (−41.93%, -0.94×10^{15} molecules/cm^2), BGD (−33.45%, -0.78×10^{15} molecules/cm^2), SGP (−23.44%, -1.24×10^{15} molecules/cm^2), and IND (−22.16%, -0.54×10^{15} molecules/cm^2), which strictly maintained nationwide lockdown throughout the study period (Fig. 5b). In both phases, TSL observed an increase in the average NO_2 levels (31.75% to 76%) amid nationwide C-19 lockdown because the duration of the lockdown was very short (March 19 to April 19, 2020), which was probably not enough to affect the atmospheric NO_2 density.

Fig. 4. Geospatial distribution of atmospheric CO surface concentration, CO near-source emission, and O_3 total column concentration in the study area at two phases during BAU and C-19 lockdown settings (column 1 and column 2). The geospatial data of C-19 lockdown (column 2) was compared with the same period of the previous year (BAU) (column 1) and presented in Column 3.

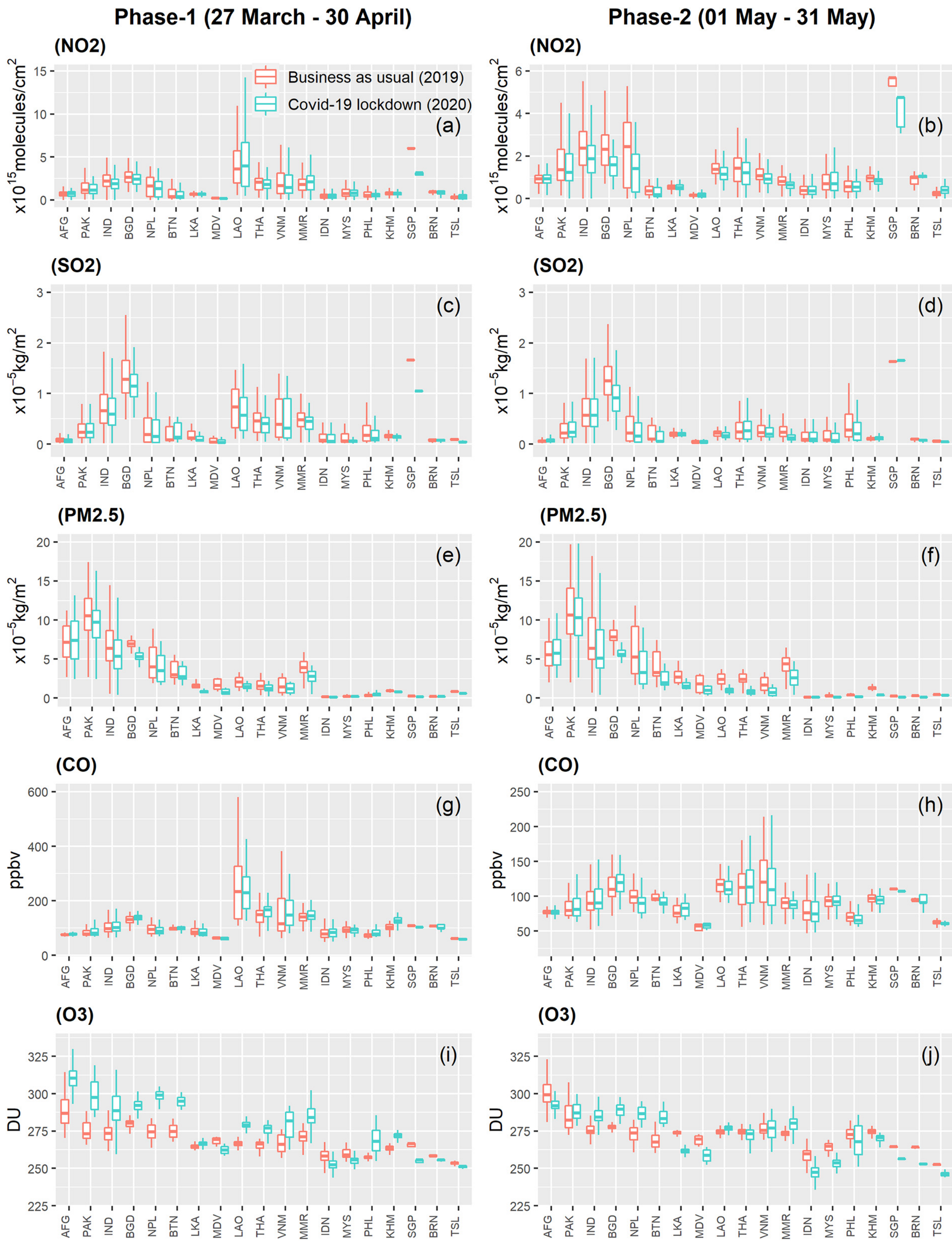

Fig. 5. Comparison of NO_2 (a and b), SO_2 (c and d), $PM_{2.5}$ (e and f), CO (g and h), and O_3 (i and j) between C-19 lockdown and BAU settings over selected cities in the study area. Statistical analysis was performed using R 4.0.2 (R Core Team, 2019).

Despite enforcement of several lockdown measures by the countries of the study area during the COVID-19 pandemic, they didn't observe the same trend of change in atmospheric SO_2 average column density during lockdown compared to the BAU of the previous year. Similar to the scenario of NO_2, the countries that implemented nationwide to a region-wise halt in several economic activities, especially the transportation and industrial activities, the major sources of SO_2 emission to the atmosphere, experienced a reduction of atmospheric SO_2 column density during lockdown. For example, compared to the same period of 2019, TSL, MYS, SGP, LKA, and NPL overserved 39.32%, 21.92%, 16.32%, 10.04%, and 7.34%, respectively, reduction in the average column density of the atmospheric SO_2 during lockdown. In phase-1, highest reduction was observed in TSL (−57.96%, -3.07×10^{-5} kg/m^2), followed by MYS (−35%, -4.92×10^{-5} kg/m^2), LKA (−28.60%, -4.87×10^{-5} kg/m^2), and SGP (−27.68%, -57.93×10^{-5} kg/m^2) (Fig. 5c). On the other hand, MMR exhibited the highest reduction (−36.47%, -2.66×10^{-5} kg/m^2) of atmospheric SO_2 average column density in phase-2 (Fig. 5d). However, four countries such as PAK, IDN, BGD, and IND didn't experience any reduction in atmospheric SO_2 column density, rather represented a modest increase in both phases with an average increase of 19.73%, 5.88%, 5.60%, and 4.32%, respectively, compared to the previous corresponding phases of BAU. The plausible causes behind this could be: constant intra-city vehicular movement was in practice due to poor implementation of lockdown measures at field level (i.e., in India, a huge number of migrant worker's movement using private and public transportation was carried out amid lockdown), late lockdown enforcement as seen in the case of IND (Fig. 2), and no suspension of industrial activities (IDN). Additionally, lifting lockdown measures before May 31, 2020 in few countries (i.e., Pakistan and Thailand took out lockdown measures before May 31, 2020 (Fig. 2)) might be contributed to the increase of SO_2 emission through resuming industries and public transports.

The average $PM_{2.5}$ markedly reduced in virtually all countries except for AFG in both phases and BRN and PHL in phase-1. All these three countries did not enforce rigid national lockdowns instead moved to region-wise lockdowns (AFG) or city-wise lockdowns (PHL), while BRN did not impose any lockdown. In phase-1 of C-19 lockdown, maximum reduction of average $PM_{2.5}$ was observed in MDV (−54%,

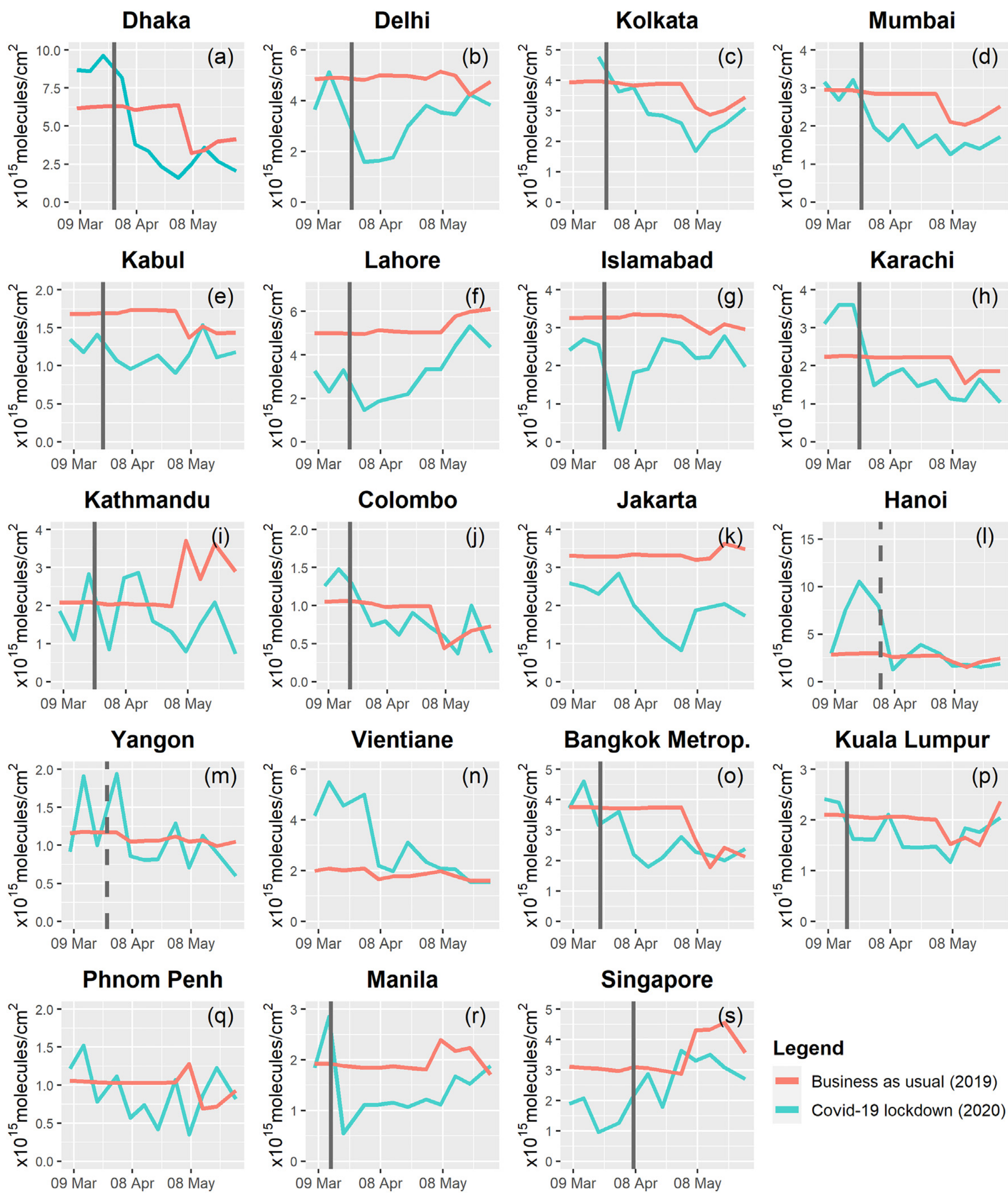

Fig. 6. Comparison of tropospheric NO_2 mean column density between C-19 lockdown and BAU settings over selected cities in the study area. The vertical black colored solid and dashed lines indicate the dates at which the COVID-19 induced strict lockdown measures and nation-wide isolation, respectively, were imposed at the cities. Statistical analysis was performed using R 4.0.2 (R Core Team, 2019).

-0.96×10^{-5} kg/m^2), followed by LKA (−46.12%, -0.73×10^{-5} kg/m^2) and SGP (−33.58%, -0.08×10^{-5} kg/m^2), compared to phase-1 of BAU (Fig. 5e). In phase-2 of C-19 lockdown, the reduction was intensified compared to the same phase of BAU, and a maximum 71% fall of average $PM_{2.5}$ was noticed in KHM (-0.92×10^{-5} kg/m^2). During this phase other countries which observed significant decline in average $PM_{2.5}$ include THA (−66.72%, -1.60×10^{-5} kg/m^2), LAO (−58.42%, -1.38×10^{-5} kg/m^2), VNM (−55.55%, -1.00×10^{-5} kg/m^2), SGP (−53.94%, -0.14×10^{-5} kg/m^2), and MYS (−53.34%, -0.16×10^{-5} kg/m^2) (Fig. 5f). Compared to BAU, the countries that observed less reduction in average $PM_{2.5}$ column density during lockdown include PAK (−8.21%), IND (−14.22%), IDN (−14.95%), TSL (−19.92%), and BGD (−25.81%). The less fall of atmospheric particulate matter, especially in BGD, PAK, and IND, maybe a consequence of large-scale burning of post-harvested agricultural wastes and exorbitant burning of coal in brick kilns throughout the year (Bhuvaneshwari et al., 2019; Kumar and Joshi, 2013; Rahman et al., 2020).

The C-19 induced lockdown measures as imposed by the countries also affected the atmospheric concentration of the CO, which is considered as one of the major greenhouses gases. Though the lifetime of this gas is very short in the atmosphere, the rise of its concentration induced from the burning of hydrocarbons and biofuels can be toxic to human health. In spite of an overall increase of CO concentration during lockdown compared to the previous year, few countries consistently represented a decrease in both phases during lockdown. In the study area, seven countries showed a reduction in phase-1, where TSL exhibited the highest 5% reduction (−3.11 ppbv), followed by SGP (−4.82%), NPL (−4.74%), and LKA (−4.37%) (Fig. 5g). The fall of atmospheric CO concentration was escalated in phase-2, while 12 countries showed an average reduction in CO concentration during lockdown compared to the corresponding BAU of 2019. Among these countries, NPL exhibited highest reduction (−10.12%, −10.22 ppbv) in phase-2, followed by VNM (−5.43%, −6.66 ppbv), BTN (−5.07%, −4.85 ppbv), and PHL (−4.95%, −3.63 ppbv) though BTN, PHL, and VNM showed an increase in the first phase (Fig. 5h). Similar to the case of SO_2, three countries such as BGD, PAK, and IND consistently reported an increase of atmospheric CO concentration amid C-19 lockdown. In both analysis phases, Cambodia (KHM), which didn't impose hard lockdown over CO emission sources (i.e., vehicles movement, industrial and processing activities, etc.) (Fig. 2), showed the highest rise of CO concentration (23.89% in phase-1 and 11.16% in phase-2) during C-19 lockdown compared to the previous BAU.

The country-scale assessment of O_3 concentration showed an overall increase in 13 countries in phase-1 and seven countries in phase-2 when compared to the BAU in the corresponding phases. From this analysis, it was evidenced that the countries that implemented strict C-19 lockdown protocols experienced increased O_3 level in the lockdown phases. The highest increase in concentration of O_3 in phase-1 was observed in NPL (8.95%), PAK (8.85%), and AFG (7.73%) when compared to BAU (Fig. 5i). In phase-2 however, this increase decelerated while the maximum increase was estimated in BTN (5.79%) and NPL (4.98%) (Fig. 5j). Conversely, a significant reduction in O_3 concentration was observed in LKA (4.49%), IDN (4.40%), MYS (4.20%), and BRN (4.20%) in phase-2 compared to the corresponding phase of BAU (Fig. 5j). Therefore, it is evident that this sudden rise in ozone in phase-1 and subsequent sharp fall in phase-2 may be attributed to the strict lockdown in phase-1 and gradual relaxing of the measures in phase-2. It is established that there is an inverse relationship between the concentration of NO_2 and O_3 despite the fact that NO_2 is a major precursor of O_3 formation along with VOCs (Jhun et al., 2014). Analyzing the NO_2 concentrations in the same period, we found that the same countries that exhibited highest increase in O_3 concentrations in phase-1 (i.e. NPL, PAK, and AFG) also observed high decrease in NO_2 concentrations (i.e., NPL, PAK, and AFG). However, there are exceptions, such as SGP showed drastic decreases in both NO_2 and O_3 as well. This phenomenon was not consistent in phase-2, where countries that had decreasing levels of NO_2 (i.e., BGD and NPL) hadn't observed proportionate increase in O_3. This might be a consequence of gradual opening of NO_2 emission sources in these countries during phase-1. A good association between $PM_{2.5}$ decreasing and O_3 increasing was observed in our study, which is aligned with the recent studies such as MMR, VNM, THA, BGD, and IND showed marked reduction in $PM_{2.5}$ (−28.65%, −23.69%, −22.93%, −22.36%, and −14.83%, respectively) during phase-1 of C-19 lockdown, which also represented increased O_3 concentration in that phase. These countries showed a further drop in the $PM_{2.5}$ level with a moderate increase in O_3 concentration in phase-2. However, country to country variation of the fluctuation of O_3 concentration might be affected by the varying types of lockdown measures with different lengths of implementation period in the study area. In addition, meteorological factors might have influenced the production of O_3 in the study area, which requires further study to understand.

3.3. Effects on air quality (NO_2) over 19 selected cities

Fig. 6 represents the temporal comparison of tropospheric NO_2 mean column density (molecules/cm^2) over 19 cities of the SA and SEA between C-19 lockdown (March 27–May 31, 2020) and BAU (March 27–May 31, 2019) settings. As presented in Fig. 2, most of the countries in the study area imposed tight nationwide lockdown initiatives except few countries which followed a relaxed and other types of contingency measures such as partial lockdown of the affected cities, social distancing, and different degrees of community quarantines. The lockdown measures were imposed with the aim to contain the new coronavirus contagion by limiting human movements and mass gathering. Among various measures the suspension of air traffic, limiting road traffic, and shutting down of industries are the major ones that affected NO_2 emission to the atmosphere. As shown in Fig. 6, the effect of C-19 lockdown measures on the atmospheric NO_2 density was highly distinguished in the studied cities between C-19 lockdown and BAU settings. Furthermore, all the cities represented certain scales of reduction in NO_2 density in the lower atmosphere throughout the C-19 lockdown period (March 27–May 31, 2020).

The intra-period (C-19 lockdown- March 27 to May 31, 2020) analysis of weekly average data represented a sharp fall of NO_2 density right after the imposition of C-19 lockdown measures in most of the cities though it didn't continue with the same reduction trend on the following weeks (Table 3). For example, the highest 87.45% (from 2.55 ×

Table 3
Changes of tropospheric NO_2 column density between C-19 lockdown and BAU settings (column 3) and changes of weekly mean NO_2 (column 4) during lockdown compared to the date of C-19 lockdown implementation in the corresponding city. The negative values indicate a decrease in tropospheric NO_2 density in the respective analysis periods.

Region	City	C-19 vs BAU setting (overall change in %)	During C-19 setting (overall change in %)
SA	Delhi	−36.79	−19.74
	Kolkata	−21.64	−41.07
	Mumbai	−29.33	−48.88
	Kabul	−11.2	−20.33
	Lahore	−34.35	−4.7
	Islamabad	−27.32	−19.13
	Karachi	−23.7	−59.29
	Dhaka	−40.56	−65.25
	Kathmandu	−40.99	−43.11
	Colombo	−30.73	−46.79
SEA	Jakarta	−46.87	−22.61
	Hanoi	−45.79	−72.03
	Yangon	−23.85	0.78
	Vientiane	−5.07	−46.52
	Bangkok Metropolis	−11.28	−25.37
	Kuala Lumpur	−23.45	1.91
	Phnom Penh	−23.25	2.42
	Singapore	−38.25	38.1
	Manila	−24.02	140.2

10^{15} molecules/cm^2 to 3.2×10^{14} molecules/cm^2) reduction was observed in Islamabad on the first week after the imposition of the C-19 lockdown on May 24, 2020 (Fig. 6g). Similarly, Hanoi recorded 83.90% (from 7.95×10^{15} molecules/cm^2 to 1.28×10^{15} molecules/cm^2) fall, the second highest fall in atmospheric NO_2 density among the studied cities on the first week after the nationwide isolation was executed on April 1, 2020 (Fig. 6i). On the same first week, 50%–70% reduction was observed in four other cities such as Kathmandu (69.96%, Fig. 6i), Karachi (58.61%, Fig. 6h), Delhi (57.26%, Fig. 6a), and Lahore (55.89%, Fig. 6f), which imposed nationwide C-19 lockdown from March 24 to 25, 2020. Besides, Mumbai (38.94%, Fig. 6d) and Colombo (42.19%, Fig. 6j) experienced around 40% reduction in the first week after the enforcement of nationwide C-19 lookdown measures (March 20 to 25, 2020). In few cities, a significant fall in NO_2 density was observed from the second week (April 1 to 7, 2020) after the imposition of lockdown measures which included Jakarta (12.55%, Fig. 6k), Bangkok Metropolis (30.50%, Fig. 6o), and Phnom Penh (26.92%, Fig. 6q). However, there were no reductions observed in Manila (Fig. 6r) and Singapore (Fig. 6s) during the C-19 lockdown setting as their contingency measures were hardly imposed over the emission sources. In the entire C-19 lockdown period, a maximum overall reduction in NO_2 density in the atmosphere was estimated in Hanoi (72%) followed by Dhaka (65.25%), Karachi (59.29%), Mumbai (48.88%), and Colombo (46.78%) compared to the pre-C-19 lockdown setting. In the intra-period of assessment, the least overall decrease was observed in Lahore (4.70%) whereas Kuala Lumpur, Phnom Penh, Manila, and Singapore showed an overall increase in NO_2 density in the atmosphere though the levels were below than the weekly average values of BAU setting of 2019 (Fig. 6p–s).

The inter-period (between C-19 and BAU settings) comparison represented that eight cities experienced 30%–46.87% (Jakarta — 46.87%, Hanoi — 45.79%, Kathmandu — 40.99%, Dhaka — 40.56%, Singapore — 38.25%, Delhi — 36.79%, Lahore — 34.35%, and Colombo — 30.73%) maximum overall reduction in mean tropospheric NO_2 density during the C-19 lockdown setting compared to the BAU setting (Table 3). Among these cities, five cities are from SA and three are from SEA countries, which included the closing of industrial and processing activities, suspension of all modes of international and inter-district transportations, and imposition of stay-at-home in their C-19 lockdown measures. The other ten cities exhibited an 11% to 30% fall in overall NO_2 density, where Vientiane of Laos showed the least reduction (5.07%) in the C-19 lockdown setting compared to the BAU setting over the study period.

The overall analysis revealed that the COVID-19 induced lockdown measures exerted an immediate effect on the reduction of pollutants level, except O3, in the atmosphere compared to the business as usual of 2019. However, these changes were seemed ephemeral and started to return to the previous state upon the gradual lifting of those measures. For example, the level of NO_2 began to increase in the atmosphere from the end of April 2020 in most of the cities of Bangladesh, India, and Pakistan, although strict lockdown measures were being officially continued in those countries till the end of May 2020 following several extensions. A similar increasing trend in NO_2 density was also observed in other cities (i.e., Manila, Singapore, Bangkok Metropolis, Kuala Lumpur, Phnom Penh, and Colombo) in the study area after certain dates. This increasing trend of certain pollutants was probably the result of the weakening of the lockdown measures or reopening of emission sources in those cities. However, few cities such as Kolkata, Karachi, Mumbai, and Jakarta experienced a long-lasting reduction of NO2 which could be the result of effective implementation of the lockdown measures throughout the period and its extension till the end of June to July (i.e., In Kolkata and Mumbai the lockdown was extended till July 31, 2020). Finally, it can be concluded that the local variations in COVID-19 induced lockdown policies, measures, timelines, and effectiveness in implementation were the major factors that worked behind the dramatic changes of pollutants in the atmosphere during this pandemic.

Since the horizontal and vertical movements of pollutants in the air are controlled by the air circulation, the NCEP/NCAR reanalysis of mean surface wind speed (m/s) was investigated for the months of BAU and C-19 settings (Fig. 7). The spatial distribution of surface wind speed for the studied months reflected the persistence of similar clam to light breeze (0.5–3.3 m/s) on the Beaufort scale in the study area, characterized by the vertical rise of smokes (clam), the direction shown by the smoke drift (light air) to wind vane moved by wind (light breeze). In Fig. 7, the comparison of the surface wind speed of C-19 lockdown months with the corresponding months of BAU, 2019 showed a very similar surface wind pattern in the corresponding months with negligible inter-period differences. Hence, it can be concluded that the

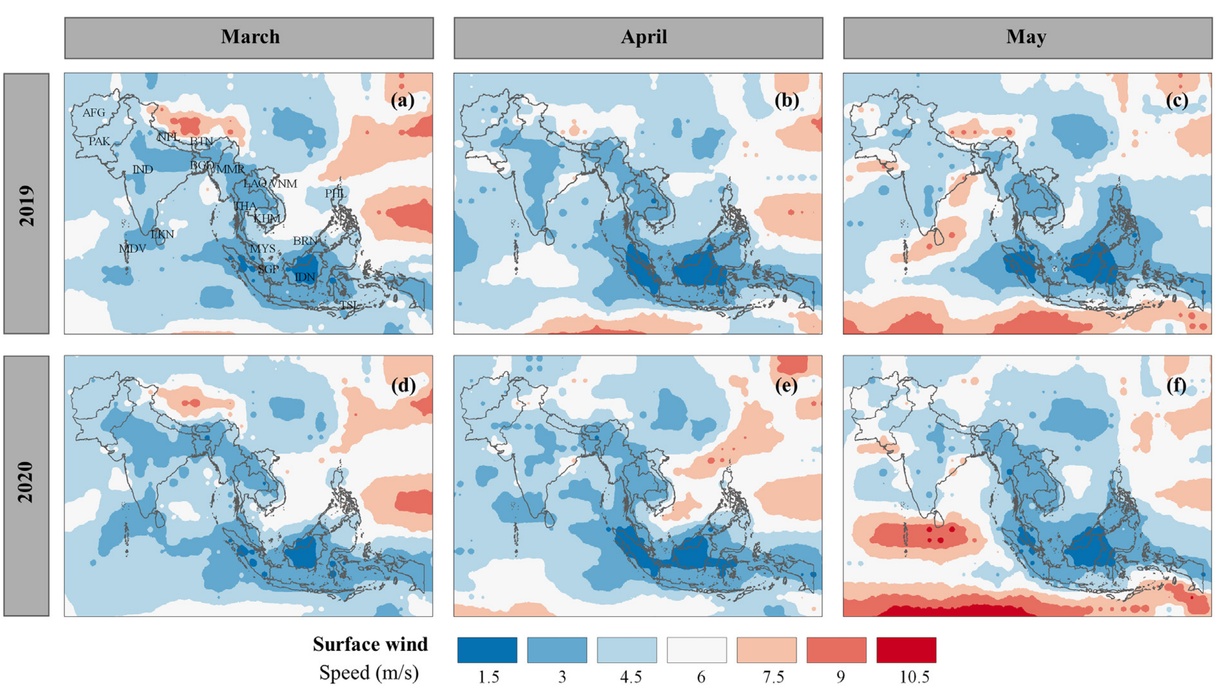

Fig. 7. Spatial distribution of average surface wind speed (m/s) in the months of BAU (a, b, and c) and C-19 lockdown periods (d, e, and f).

comparison of air pollutants distribution between BAU and C-19 lockdown was logical as the similar air circulation patterns were persisted in both BAU and C-19 lockdown periods, and thus the distribution of pollutants in the atmosphere during these two periods was similarly affected by the large scale air circulation.

3.4. Limitations and future studies

This assessment was conducted wholly based on the open-source data and freely available documentation on COVID-19 mitigation measures. Hence, the limitations of this study are mostly associated with the characteristics of geospatial data and accessibility to the COVID-19 related resources. The limitation in the review of the lockdown measures induced by the language barrier, which did not allow us to include more detailed lockdown measures imposed by the countries on the cities or on the specific economic sectors. Moreover, the changes that happened in the emission sectors such as industrial production, transportation, agriculture, etc. of the countries during the lockdown period were not included in the analysis due to the lacking of freely available information resources. Since we extracted global gridded data of pollutants from the Giovanni, these were with different spatial resolutions ranging from 27.75 km (0.25°) to 70 km (0.625°), approximately. These coarse spatial resolution datasets hardly allowed us to include relatively smaller cities in the assessment, despite with higher pollution level. We resampled the dataset to 1 km spatial resolution for performing city-scale assessment. Though the resampling method didn't affect the values of the centered pixels, it still affected the values of the edge pixels at a negligible level.

In this assessment, we considered a common lockdown period (March 27–May 31, 2020) that was operational in all the countries almost at the same time, though few countries like India, Bangladesh, and Pakistan extended the lockdown measures in their several districts or regions till the end of June. Therefore, the future study can address these data limitations and extend the assessment period to understand the long term effects of the enforcement of COVID-19 induced lockdown measures on air pollution level. The distribution and changes of the levels of air pollutants may also be influenced by meteorological factors such as air temperature, relative humidity, large-scale wind pattern, air pressure, etc. (Huang et al., 2020). This current research only addressed the scenario of large-scale surface wind patterns in both BAU and C-19 lockdown periods. Other meteorological factors can be investigated in further research to understand their effects on the fluctuation of air pollutants during the C-19 lockdown period.

4. Conclusion

COVID-19 pandemic has brought an unprecedented effect on global air quality. Several countries have reported a significant reduction in certain air pollutants due to a suspension of economic activities, especially the temporary shutdown of industrial and manufacturing operations, suspension of road and air traffic (except goods and emergency services), and halt in construction activities during C-19 lockdown periods. The systematic review of lockdown measures and the spatio-temporal analysis applied in this study together has presented a methodological framework for analyzing the effect of this pandemic mitigation measures on the regional-scale air quality. The results showed that overall air quality in the study area was improved significantly during the lockdown as at least 50% of the study area went through a notable reduction of atmospheric NO_2, SO_2, and $PM_{2.5}$ column densities due to the implementation of several COVID-19 induced lockdown measures. However, the O_3 concentration increased unexpectedly in 80% of the study area, approximately when compared to BAU. This ozone amplification was most likely due to the decrease in NO_2 and $PM_{2.5}$ concentrations during the lockdown.

The country-scale analysis represented the change of the pollutants in different countries, which varied country to country based on the type and duration of the imposition of C-19 lockdown measures. While most of the countries experienced a reduction in certain pollutants, few countries observed a contrasting scenario such as LAO, MYS, MMR, BRN, and MDV, which showed a rise of the atmospheric NO_2 level during the C-19 lockdown setting compared to the same BAU setting. Such exceptions were noticed for the countries which didn't impose nationwide stringent lockdown measures or lifted the lockdown after a short period of implementation. The city-scale analysis also represented a similar scenario where the trends of pollutant (NO2) in the air started to increase with the gradual lifting of the lockdown measures. This fluctuation of air pollutants during the COVID-19 period indicates that the improvement of air quality is an immediate consequence of the reduction of emissions owing to the enforcement of C-19 lockdown measures, which is not sustainable for a long time. This finding is aligned with Wang et al. (2020a), who mentioned that the effect of the temporary shutdown in China on lowering air pollution is transient. Furthermore, the amplification of secondary pollutants, especially O3, in many countries during the lockdown, as explored in this research, makes the improvement of air quality questionable.

However, the findings of this study, including the structured review of country-based C-19 mitigation measures, can strengthen future research by providing an information base. Our proposed analytical framework using open-source software packages and freely available model/satellite-based estimations offers a flexible approach, which can be replicated to any other study area. The change in air quality during this pandemic may be impermanent, but the effects of C-19 lockdown measures on air pollution explored in this research have shown that it is possible to improve air quality for the long term if a joint-emission-control plan is strictly implemented by the governments in the study region rather than sporadic and abrupt interventions.

Funding

This research did not receive any specific grant from funding agencies in the public, commercial, or not-for-profit sectors.

CRediT authorship contribution statement

Sanjoy Roy: Conceptualization, Methodology, Software, Visualization, Validation, Writing - original draft, Supervision. **Monojit Saha:** Data curation, Validation, Writing - review & editing. **Bandhan Dhar:** Data curation, Validation, Writing - review & editing. **Santa Pandit:** Writing - original draft. **Rubaiya Nasrin:** Visualization.

Declaration of competing interest

The authors declare that they have no known competing financial interests or personal relationships that could have appeared to influence the work reported in this paper.

Acknowledgments

Erathdata-NASA (Giovanni platform) is sincerely acknowledged for providing air pollution datasets.

Appendix A. Supplementary material

Supplementary material to this article can be found online at https://doi.org/10.1016/j.scitotenv.2020.144009.

References

van Aardenne, J.A., Carmichael, G.R., Levy II, H., Streets, D., Hordijk, L., 1999. Anthropogenic NOx emissions in Asia in the period 1990–2020. Atmos. Environ. 33 (4), 633–646. https://doi.org/10.1016/S1352-2310(98)00110-1.

Acter, T., Uddin, N., Das, J., Akhter, A., Choudhury, T.R., Kim, S., 2020. Evolution of severe acute respiratory syndrome coronavirus 2 (SARS-CoV-2) as coronavirus disease 2019 (COVID-19) pandemic: a global health emergency. Sci. Total Environ. 730, 138996. https://doi.org/10.1016/j.scitotenv.2020.138996.
Anwar, S., Nasrullah, M., Hosen, M.J., 2020. COVID-19 and Bangladesh: challenges and how to address them. Front. Public Health 8, 154. https://doi.org/10.3389/fpubh.2020.00154.
Arunachalam, M.A., Halwai, A., 2020. An analysis of the ethics of lockdown in India. Asian Bioethics Rev. https://doi.org/10.1007/s41649-020-00133-3.
Bengal Institute for Architecture, Landscapes and Settlements (BI), 2020. An atlas of COVID-19.Available online:. https://bengal.institute/covid19/ (accessed 07.19.20).
Bhattacharya, S.C., Salam, P.A., Sharma, M., 2000. Emissions from biomass energy use in some selected Asian countries. Energy 25 (2), 169–188. https://doi.org/10.1016/S0360-5442(99)00065-1.
Bhuvaneshwari, S., Hettiarachchi, H., Meegoda, J.N., 2019. Crop residue burning in India: policy challenges and potential solutions. Int. J. Environ. Res. Public Health 16. https://doi.org/10.3390/ijerph16050832.
Burke, M., 2020. COVID-19 reduces economic activity, which reduces pollution, which saves lives.Available online:. http://www.g-feed.com/2020/03/covid-19-reduces-economic-activity.html (accessed 03/06/2020).
CAMS, 2020. Amid coronavirus outbreak: Copernicus monitors reduction of particulate matter (PM2.5) over China. Available online:. https://atmosphere.copernicus.eu/amid-coronavirus-outbreak-copernicusmonitors-reduction-particulate-matter-pm25-over-china.
Carbon Brief, 2020. As China Battles One of the Most Serious Virus Epidemics of the Century, the Impacts on the Country's Energy Demand and Emissions Are Only Beginning to Be Felt.
Centre for Science and Environment (CSE), 2020. Ozone levels increased during lockdown, says CSE's new analysis of air pollution levels in 22 cities across India. Available online:. https://www.cseindia.org/analysis-of-air-pollution-levels-in-22-cities-across-india-10231.
Dang, R., Liao, H., 2019. Radiative forcing and health impact of aerosols and ozone in China as the consequence of clean air actions over 2012–2017. Geophys. Res. Lett. 46, 12511–12519. https://doi.org/10.1029/2019GL084605.
Duncan, B.N., Prados, A.I., Lamsal, L.N., Liu, Y., Streets, D.G., Gupta, P., Hilsenrath, E., Kahn, R.A., Nielsen, J.E., Beyersdorf, A.J., Burton, S.P., Fiore, A.M., Fishman, J., Henze, D.K., Hostetler, C.A., Krotkov, N.A., Lee, P., Lin, M., Pawson, S., Pfister, G., Pickering, K.E., Pierce, R.B., Yoshida, Y., Ziemba, L.D., 2014. Satellite data of atmospheric pollution for U.S. air quality applications: examples of applications, summary of data end-user resources, answers to FAQs, and common mistakes to avoid. Atmos. Environ. 94, 647–662. https://doi.org/10.1016/j.atmosenv.2014.05.061.
Dutheil, F., Baker, J.S., Navel, V., 2020. COVID-19 as a factor influencing air pollution? Environ. Pollut. 263, 2019–2021. https://doi.org/10.1016/j.envpol.2020.114466.
ESA, 2020. COVID-19: nitrogen dioxide over China.Available online:. https://www.esa.int/Applications/Observing_the_Earth/Copernicus/Sentinel-5P/COVID-19_nitrogen_dioxide_over_China (accessed 04/04/2020).
Fioletov, V.E., McLinden, C.A., Krotkov, N., Moran, M.D., Yang, K., 2011. Estimation of SO_2 emissions using OMI retrievals. Geophys. Res. Lett. 38, 1–5. https://doi.org/10.1029/2011GL049402.
Ghauri, B., Lodhi, A., Mansha, M., 2007. Development of baseline (air quality) data in Pakistan. Environ. Monit. Assess. 127, 237–252. https://doi.org/10.1007/s10661-006-9276-8.
GMAO, 2015. MERRA-2 tavgM_2d_chm_Nx: 2d, Monthly Mean, Time-averaged, Single-level, Assimilation, Carbon Monoxide and Ozone Diagnostics V5.12.4, Greenbelt. https://doi.org/10.5067/WMT31RKEXK8I.
Hopke, P.K., Cohen, D.D., Begum, B.A., Biswas, S.K., Ni, B., Pandit, G.G., Santoso, M., Chung, Y.S., Davy, P., Markwitz, A., Waheed, S., Siddique, N., Santos, F.L., Pabroa, P.C.B., Seneviratne, M.C.S., Wimolwattanapun, W., Bunprapob, S., Vuong, T.B., Duy Hien, P., Markowicz, A., 2008. Urban air quality in the Asian region. Sci. Total Environ. 404, 103–112. https://doi.org/10.1016/j.scitotenv.2008.05.039.
Hu, B., Zhao, X., Liu, H., Liu, Z., Song, T., Wang, Y., Tang, L., Xia, X., Tang, G., Ji, D., Wen, T., Wang, L., Sun, Y., Xin, J., 2017. Quantification of the impact of aerosol on broadband solar radiation in North China. Sci. Rep. 7, 1–8. https://doi.org/10.1038/srep44851.
Huang, J., Zhang, L., Liu, X., Wei, Y., Liu, C., Lian, X., Huang, Z., Chou, J., Liu, X., Li, X., Yang, K., Wang, J., Liang, H., Gu, Q., Du, P., Zhang, T., 2020. Global prediction system for COVID-19 pandemic. Sci. Bull. https://doi.org/10.1016/j.scib.2020.08.002 (in press).
Ilyas, S.Z., Khattak, A.I., Nasir, S.M., Qurashi, T., Durrani, T., 2010. Air pollution assessment in urban areas and its impact on human health in the city of Quetta, Pakistan. Clean Techn. Environ. Policy 12, 291–299. https://doi.org/10.1007/s10098-009-0209-4.
IQAir, 2019. 2019 world air quality report: region and city $PM_{2.5}$ ranking. Available online: . https://www.iqair.com/world-most-polluted-countries.
Jain, S., Sharma, T., 2020. Social and travel lockdown impact considering coronavirus disease (Covid-19) on air quality in megacities of India: present benefits, future challenges and way forward. Aerosol Air Qual. Res. 20, 1222–1236. https://doi.org/10.4209/aaqr.2020.04.0171.
Jhun, I., Coull, B.A., Zanobetti, A., Koutrakis, P., 2014. The impact of nitrogen oxides concentration decreases on ozone trends in the USA. Air Qual. Atmos. Heal. 8, 283–292. https://doi.org/10.1007/s11869-014-0279-2.
Kalnay, et al., 1996. The NCEP/NCAR 40-year reanalysis project. Bull. Am. Meteorol. Soc. 77, 437–470.
Kanniah, K.D., Kamarul Zaman, N.A.F., Kaskaoutis, D.G., Latif, M.T., 2020. COVID-19's impact on the atmospheric environment in the Southeast Asia region. Sci. Total Environ. 736. https://doi.org/10.1016/j.scitotenv.2020.139658.
Kaplan, J., Frias, L., Johnsen, M., 2020. Countries around the world are reopening — here's our constantly updated list of how they're doing it and who remains under lockdown. Bus. Insid. Available online:. https://www.businessinsider.com/countries-on-lock-down-coronavirus-italy-2020-3.
Kerimray, A., Baimatova, N., Ibragimova, O.P., Bukenov, B., Kenessov, B., Plotitsyn, P., Karaca, F., 2020. Assessing air quality changes in large cities during COVID-19 lockdowns: the impacts of traffic-free urban conditions in Almaty, Kazakhstan. Sci. Total Environ. 730, 139179. https://doi.org/10.1016/j.scitotenv.2020.139179.
Kovač-Andrić, E., Radanović, T., Topalović, I., Marković, B., Sakač, N., 2013. Temporal variations in concentrations of ozone, nitrogen dioxide, and carbon monoxide at Osijek, Croatia. Adv. Meteorol. 2013. https://doi.org/10.1155/2013/469786.
Kumar, P., Joshi, L., Kaechele, H., 2013. Pollution caused by agricultural waste burning and possible alternate uses of crop stubble: A case study of Punjab. In: Nautiyal, S., Rao, K.S., Raju, K.V., Schaldach, R. (Eds.), Knowledge Systems of Societies for Adaptation and Mitigation of Impacts of Climate Change. Springer Berlin Heidelberg, Berlin, Heidelberg, pp. 367–385 https://doi.org/10.1007/978-3-642-36143-2_22.
Le, T., Wang, Y., Liu, L., Yang, J., Yung, Y.L., Li, G., Seinfeld, J.H., 2020. Unexpected air pollution with marked emission reductions during the COVID-19 outbreak in China. Science 369, 702–706. https://doi.org/10.1126/science.abb7431.
Lefohn, A.S., Malley, C.S., Smith, L., Wells, B., Hazucha, M., Simon, H., Naik, V., Mills, G., et al., 2018. Tropospheric ozone assessment report: global ozone metrics for climate change, human health, and crop/ecosystem research. Elem. Sci. Anth. 6, 28. https://doi.org/10.1525/elementa.279.
Li, L., Li, Q., Huang, L., Wang, Q., Zhu, A., Xu, J., Liu, Ziyi, Li, H., Shi, L., Li, R., Azari, M., Wang, Y., Zhang, X., Liu, Zhiqiang, Zhu, Y., Zhang, K., Xue, S., Ooi, M.C.G., Zhang, D., Chan, A., 2020. Air quality changes during the COVID-19 lockdown over the Yangtze River Delta Region: an insight into the impact of human activity pattern changes on air pollution variation. Sci. Total Environ. 732. https://doi.org/10.1016/j.scitotenv.2020.139282.
Lian, X., Huang, J., Huang, R., Liu, C., Wang, L., Zhang, T., 2020. Impact of city lockdown on the air quality of COVID-19-hit of Wuhan city. Sci. Total Environ. 742, 140556. https://doi.org/10.1016/j.scitotenv.2020.140556.
Luong, L.M.T., Sly, P.D., Thai, P.K., Phung, D., 2019. Impact of ambient air pollution and wheeze-associated disorders in children in Southeast Asia: a systematic review and meta-analysis. Rev. Environ. Health 34 (2). https://doi.org/10.1515/reveh-2018-0079.
Ma, Y., Zhao, Y., Liu, J., He, X., Wang, B., Fu, S., Yan, J., Niu, J., Zhou, J., Luo, B., 2020. Effects of temperature variation and humidity on the death of COVID-19 in Wuhan, China. Sci. Total Environ. 724, 138226. https://doi.org/10.1016/j.scitotenv.2020.138226.
Mahato, S., Pal, S., Ghosh, K.G., 2020. Effect of lockdown amid COVID-19 pandemic on air quality of the megacity Delhi, India. Sci. Total Environ. 730, 139086. https://doi.org/10.1016/j.scitotenv.2020.139086.
Mandal, I., Pal, S., 2020. COVID-19 pandemic persuaded lockdown effects on environment over stone quarrying and crushing areas. Sci. Total Environ. 732, 139281. https://doi.org/10.1016/j.scitotenv.2020.139281.
Motalib, Mohammad Abdul, D. Lasco, Rodel, P. Pacardo, Enrique, Rebancos, C., Dizon, J., 2015. Health impact of air pollution on Dhaka City by different technologies Brick Kilns. Int. J. Techno. Enhanc. Emerg. Eng. Res.
Muhammad, S., Long, X., Salman, M., 2020. COVID-19 pandemic and environmental pollution: a blessing in disguise? Sci. Total Environ. 728, 138820. https://doi.org/10.1016/j.scitotenv.2020.138820.
Nakada, L.Y.K., Urban, R.C., 2020. COVID-19 pandemic: impacts on the air quality during the partial lockdown in São Paulo state, Brazil. Sci. Total Environ. 730, 139087. https://doi.org/10.1016/j.scitotenv.2020.139087.
Nichol, J.E., Bilal, M., Ali, A.M., Qiu, Z., 2020. Air pollution scenario over China during COVID-19. Remote Sens. 12. https://doi.org/10.3390/rs12132100.
Nickolay, A.., Lamsal, N.., Marchenko, S.V., Celarier, E.A., Bucsela, E.., Swartz, W.., Joiner, J., 2019. OMI/Aura NO_2 Cloud-screened Total and Tropospheric Column L3 Global Gridded 0.25 Degree × 0.25 Degree V3. https://doi.org/10.5067/Aura/OMI/DATA300.
Oanh, K.N.T., Upadhyay, N., Zhuang, Y.H., Hao, Z.P., Murthy, D.V.S., Lestari, P., Villarin, J.T., Chengchua, K., Co, H.X., Dung, N.T., Lindgren, E.S., 2006. Particulate air pollution in six Asian cities: spatial and temporal distributions, and associated sources. Atmos. Environ. 40, 3367–3380. https://doi.org/10.1016/j.atmosenv.2006.01.050.
Otmani, A., Benchrif, A., Tahri, M., Bounakhla, M., Chakir, E.M., El Bouch, M., Krombi, M., 2020. Impact of Covid-19 lockdown on PM_{10}, SO_2 and NO_2 concentrations in Salé City (Morocco). Sci. Total Environ. 735, 139541. https://doi.org/10.1016/j.scitotenv.2020.139541.
Oxford Covid-19 Government Response Tracker, 2020. Regional reports- East Asia and Pacific and South Asia.Available online:. https://www.bsg.ox.ac.uk/research/research-projects/coronavirus-government-response-tracker (accessed 07/06/2020).
Prados, A.I., Leptoukh, G., Lynnes, C., Johnson, J., Rui, H., Chen, A., Husar, R.B., 2010. Access, visualization, and interoperability of air quality remote sensing data sets via the Giovanni online tool. IEEE J. Sel. Top. Appl. Earth Obs. Remote Sens. 3, 359–370. https://doi.org/10.1109/JSTARS.2010.2047940.
R Core Team, 2019. The R project for statistical computing. Available online:. https://www.r-project.org/.
Rahman, M. Habibur, Al-Muyeed, Abdullah, 2005. Urban air pollution: a Bangladesh perspective. WIT Trans. Ecol. Environ. 82.
Rahman, M.M., Begum, B.A., Hopke, P.K., Nahar, K., Thurston, G.D., 2020. Assessing the $PM_{2.5}$ impact of biomass combustion in megacity Dhaka, Bangladesh. Environ. Pollut. 264, 1–11. https://doi.org/10.1016/j.envpol.2020.114798.
Saadat, S., Rawtani, D., Hussain, C.M., 2020. Environmental perspective of COVID-19. Sci. Total Environ. 728. https://doi.org/10.1016/j.scitotenv.2020.138870.
Seinfeld, J.H., Pandis, S.N., 1998. Atmospheric Chemistry and Physics. From Air Pollution to Climate Changes (Ed. 3). vol. 1998. Wiley, New York, USA ISBN: 978-1-118-94740-1.
Sharma, S., Zhang, M., Anshika, Gao, J., Zhang, H., Kota, S.H., 2020b. Effect of restricted emissions during COVID-19 on air quality in India. Sci. Total Environ. 728, 138878. https://doi.org/10.1016/j.scitotenv.2020.138878.

Shrestha, R., Shrestha, S., Khanal, P., Bhuvan, K., 2020. Nepal's first case of COVID-19 and public health response. J. Trav. Med. 27 (3). https://doi.org/10.1093/jtm/taaa024.

Sicard, P., Marco, A.D., Agathokleous, E., Feng, Z., Xu, X., Paoletti, E., Rodriguez, J.J.D., Calatayud, V., 2020. Amplified ozone pollution in cities during the COVID-19 lockdown. Sci. Total Environ. 735, 139542. https://doi.org/10.1016/j.scitotenv.2020.139542.

The Diplomat, 2020. COVID-19 in Asia: a country-by-country guide. Available online:. https://thediplomat.com/2020/04/covid-19-in-asia-a-country-by-country-guide/.

Tobías, A., Carnerero, C., Reche, C., Massagué, J., Via, M., Minguillón, M.C., Alastuey, A., Querol, X., 2020. Changes in air quality during the lockdown in Barcelona (Spain) one month into the SARS-CoV-2 epidemic. Sci. Total Environ. 726, 138540. https://doi.org/10.1016/j.scitotenv.2020.138540.

Wang, C., Horby, P.W., Hayden, F.G., Gao, G., 2020c. A novel coronavirus outbreak of global health concern. Lancet 395, 470–473. https://doi.org/10.1016/S0140-6736(20)30185-9.

Wang, L., Li, M., Yu, S., Chen, X., Li, Z., Zhang, Y., Jiang, L., Xia, Y., Li, J., Liu, W., Li, P., Lichtfouse, E., Rosenfeld, D., Seinfeld, J.H., 2020d. Unexpected rise of ozone in urban and rural areas, and sulfur dioxide in rural areas during the coronavirus city lockdown in Hangzhou, China: implications for air quality. Environ. Chem. Lett. https://doi.org/10.1007/s10311-020-01028-3.

Wang, M., Jiang, A., Gong, L., Luo, L., Guo, W., Li, C., Zheng, J., Li, C., Yang, B., Zeng, J., 2020b. Temperature significant change COVID-19 transmission in 429 cities. medRxiv https://doi.org/10.1101/2020.02.22.20025791.

Wang, P., Chen, K., Zhu, S., Wang, P., Zhanga, H., 2020a. Severe air pollution events not avoided by reduced anthropogenic activities during COVID-19 outbreak. Res. Conserv. Recycl. 158. https://doi.org/10.1016/j.resconrec.2020.104814.

WHO, 2014. 7 million premature deaths annually linked to air pollution.Available online:. https://www.who.int/mediacentre/news/releases/2014/air-pollution/en/ (accessed 30/06/2020).

WHO, 2020a. WHO Coronavirus disease (COVID-19) control dashboard.Available online:. https://covid19.who.int/?gclid=Cj0KCQjw3s_4BRDPARIsAJsyoLNA57bSwWx2UG_VMqc3SZv2YQ17yvGZXShDtgI906I0h5eDFRqyoLcaAjn9EALw_wcB (accessed 19/07/2020).

WHO, 2020b. Coronavirus disease (COVID-19) pandemic.Available online:. https://www.who.int/emergencies/diseases/novel-coronavirus-2019 (accessed 30/05/2020).

WHO, 2020c. Disease outbreak news: Novel Coronavirus – Thailand (ex-China).Available online:. https://www.who.int/csr/don/en/ (accessed 19/07/2020).

WHO. Regional Office for Europe, 2006. Air Quality Guidelines Global Update 2005: Particulate Matter, Ozone, Nitrogen Dioxide and Sulfur Dioxide. WHO Regional Office for Europe, Copenhagen https://apps.who.int/iris/handle/10665/107823. (Accessed 15 July 2020).

World Bank, 2019. Population, Total.Available online:. https://data.worldbank.org/indicator/SP.POP.TOTL?end=2019&start=2019 (accessed 19/07/2020).

Wu, F., Zhao, S., Yu, B., Chen, Y.M., Wang, W., Song, Z.G., Hu, Y., Tao, Z.W., Tian, J.H., Pei, Y.Y., Yuan, M.L., Zhang, Y.L., Dai, F.H., Liu, Y., Wang, Q.M., Zheng, J.J., Xu, L., Holmes, E.C., Zhang, Y.Z., 2020. A new coronavirus associated with human respiratory disease in China. Nature 579, 265–269. https://doi.org/10.1038/s41586-020-2008-3.

Yunus, A.P., Masago, Y., Hijioka, Y., 2020. COVID-19 and surface water quality: improved lake water quality during the lockdown. Sci. Total Environ. 731, 139012. https://doi.org/10.1016/j.scitotenv.2020.139012.

Zahangir, M., Sarker, A., Alam, M., 2001. Air pollution due to vehicle exhaust in Dhaka City. Int. Conf. on Mechanical Eng, pp. 37–42.

Zambrano-Monserrate, M.A., Ruano, M.A., Sanchez-Alcalde, L., 2020. Indirect effects of COVID-19 on the environment. Sci. Total Environ. 728. https://doi.org/10.1016/j.scitotenv.2020.138813.

Zou, B., Chen, J., Zhai, L., Fang, X., Zheng, Z., 2017. Satellite based mapping of ground $PM_{2.5}$ concentration using generalized additive modeling. Remote Sens. 9, 1–16. https://doi.org/10.3390/rs9010001.